Proximity-induced collective modes in an unconventional superconductor heterostructure

Jonathan B. Curtis,[1,2] Nicholas R. Poniatowski,[2] Amir Yacoby,[1,2] and Prineha Narang[1,*]

[1] *John A. Paulson School of Applied Sciences and Engineering,*
Harvard University, Cambridge Massachusetts 02138 USA
[2] *Department of Physics, Harvard University, Cambridge, MA 02138, USA*
(Dated: August 8, 2022)

Unconventional superconductors have been long sought for their potential applications in quantum technologies and devices. A key challenge impeding this effort is the difficulty associated with probing and characterizing candidate materials and establishing their order parameter. Here we present a platform that allows one to spectroscopically probe unconventional superconductivity in thin-layer materials *via* the proximity effect. We show that inducing an *s*-wave gap in a sample with an intrinsic *d*-wave instability leads to the formation of bound-states of quasiparticle pairs, which manifest as a collective mode in the *d*-wave channel. This finding provides a way to study the underlying pairing interactions vicariously through the collective mode spectrum of the system. Upon further cooling of the system we observe that this mode softens considerably and may even condense, signaling the onset of time-reversal symmetry breaking superconductivity. Therefore, our proposal also allows for the creation and study of these elusive unconventional states.

I. INTRODUCTION

Materials exhibiting unconventional superconductivity are key components of many proposed quantum devices. For instance, triplet superconductors may allow for the incorporation of magnetic functionalities into superconducting electronics [1, 2], as well as offering larger critical magnetic field strengths [1, 3]. Similarly, a large amount of work has been devoted towards realizing topological superconductors, such as the elusive chiral *p*-wave state [4–6]. Many of these useful unconventional states break additional symmetries, beyond global $U(1)$ symmetry, such as time-reversal symmetry [7–12].

The question of how to realize [6, 13, 14] and prepare these systems not withstanding, it is often very difficult to even characterize and verify the nature of these unconventional superconducting phases. Often, low dimensionality, low temperature scales, and complex order parameters can conspire to obscure the microscopic structure of the ground state, making the unambiguous identification of the state challenging. It has recently been emphasized that one potential solution to this problem is to use the spectrum of collective modes in the superconductor to look for signatures of the ground state order [2, 15–17]. For example, one may study the multiple different Higgs modes of an anisotropic superconductor to identify the ground state symmetry [15, 18–20]. Similarly, in the case of time-reversal symmetry breaking multicomponent [17, 21, 22] or multiband [10, 23, 24] superconductors, it has been argued that collective modes associated to the relative phase stiffnesses may also provide signatures of the time-reversal symmetry breaking.

While promising, this method is greatly restricted in its applicability. In order to support these collective modes, the material must already have two or more closely competing interactions, and if the system has a nodal order parameter there is an additional threat due to quasiparticle damping. In addition, the relevant frequency scales for these collective modes is almost always on the order of the electronic gap, and therefore usually falls within a challenging frequency range of low-to-mid THz.

In this article, we present a way to overcome these challenges in a controlled and tunable manner by using the proximity effect to build a "designer" collective mode. This collective mode can then be used to probe the order parameter of a candidate material by standard means such as Raman or tunneling spectroscopy. Further, we show that this protocol may yield a way to engineer systems which spontaneously break time-reversal symmetry, offering a way to systematically study these elusive superconducting states.

Fundamentally, our scheme relies on using a conventional bulk "substrate" superconductor to proximity induce *s*-wave superconductivity in a thin "sample" layer of unconventional superconductor which has an intrinsic instability towards pairing in a non-*s*-wave channel, as depicted in Fig. 1(a). In the presence of the proximity-induced minigap this residual interaction manifests through the formation of stable bound-states of quasiparticle pairs (note this is different from the case of a single-electron bound state [25–27]). These bound states essentially realize the Bardasis-Schrieffer, or "particle-particle exciton," collective mode [28], but in this case the sub-dominant pairing interaction is the dominant pairing interaction in the sample.

We also confirm that if the intrinsic pairing interaction in the sample is sufficiently strong, the particle-particle bound-state may itself condense, at which point the system undergoes a second phase transition into a time-reversal symmetry breaking state with a mixed order in both channels. This hierarchy of temperatures and the various regimes are shown in Fig. 1(b).

* prineha@seas.harvard.edu
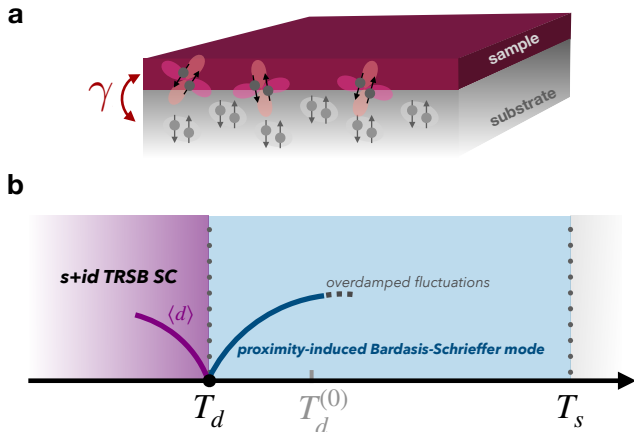
FIG. 1. (**a**) Schematic of the heterostructure under study in this work: an unconventional superconducting sample placed in proximity to a conventional bulk superconducting substrate. The two sub-systems are coupled via single-particle tunneling which occurs at the rate γ. (**b**) Phase diagram of the system. Below T_s, the substrate is superconducting and induces a minigap in the sample via the proximity effect. When this minigap becomes large enough, it converts the overdamped fluctuations of the d-wave superconducting order into a sharp collective mode. As the sample transition temperature T_d is approached, this proximitized collective mode softens and ultimately condenses out-of-phase with the substrate order parameter, spontaneously breaking time-reversal symmetry. Below T_d, the proximity-induced collective mode becomes the usual clapping mode in time-reversal symmetry breaking superconductors.

II. MODEL

For specificity, we will first demonstrate this idea by considering a concrete model where the sample has single-band spin-singlet $d_{x^2-y^2}$-wave order. In the appendix, we also consider a more complex example of f-wave triplet pairing in moiré graphene, using the model proposed in Ref. [29]; we will discuss this in more detail later since it qualitatively resembles the similar case of d-wave pairing for our purposes. Indeed, we expect that our results will largely generalize to more complex order parameters, provided they remain orthogonal to the s-wave order in the presence of the interface [30], and that the relevant order parameters commute with the normal state Bloch Hamiltonian. We leave a systematic analysis to future studies, only noting there is a potentially interesting connection between the collective mode spectra and the notion of "superconducting fitness"[31]. Additionally, for simplicity, we take the sample thickness to be thin compared to the coherence length in the out-of-plane direction, such that we may neglect the dispersion, and hence the spatial dependence of the problem, in the transverse direction.

In this case, we describe the intrinsic pairing interac-

tion in the sample by a BCS Hamiltonian

$$H_0 = \sum_{\mathbf{p}\sigma} \xi_{\mathbf{p}} c_{\mathbf{p}\sigma}^\dagger c_{\mathbf{p}\sigma}$$

$$- g_d \sum_{\mathbf{q}} \int_{\mathbf{p},\mathbf{p}'} \chi_{\mathbf{p}}^d \chi_{\mathbf{p}'}^d c_{\mathbf{p}'+\frac{1}{2}\mathbf{q},\uparrow}^\dagger c_{-\mathbf{p}'+\frac{1}{2}\mathbf{q},\downarrow}^\dagger c_{-\mathbf{p}+\frac{1}{2}\mathbf{q}\downarrow} c_{\mathbf{p}+\frac{1}{2}\mathbf{q}\uparrow},$$

$$(1)$$

with the dispersion relation $\xi_{\mathbf{p}} = \mathbf{p}^2/2m - E_F$. The second term describes the d-wave pairing interaction with center-of-mass momentum $\mathbf{q}$ and relative momentum $\mathbf{p}$, codified in the d-wave form-factor $\chi_{\mathbf{p}}^d = \sqrt{2}\cos(2\theta_{\mathbf{p}})$ (the momentum angle is measured from the x-axis).

Within mean-field theory the pairing interaction can be decoupled, yielding the standard Bogoliubov-de Gennes Hamiltonian for quasiparticles. Solving this self-consistently for the d-wave gap

$$\frac{1}{g_d}\Delta^d = \int_{\mathbf{p}} \chi_{\mathbf{p}}^d \langle c_{-\mathbf{p}\downarrow} c_{\mathbf{p}\uparrow}\rangle, \qquad (2)$$

we find that d-wave pairing sets in at a temperature $T_d^{(0)}$ which is given by the standard BCS formula in terms of the dimensionless pairing strength $\lambda_d = g_d\nu_F$ (with ν_F the density-of-states at the Fermi level), and a UV cutoff Λ of order of the characteristic frequency of whatever mediates pairing in the sample (e.g., for phonons, the Debye frequency). In this work we do not consider any changes to the intrinsic interaction due to the substrate, though this is an interesting direction for future study.

We now introduce the coupling to the substrate, which we treat as a fixed "reservoir," that doesn't experience any back-reaction due to the coupling to the sample. In particular, we assume the substrate is much thicker than the sample and the s-wave coherence length. Crucially, we also assume that the substrate transition temperature T_s is much larger than the intrinsic transition temperature in the sample $T_d^{(0)}$, or equivalently that the substrate superconducting gap $|\Delta_s|$ has largely saturated once the temperature reaches $T \sim T_d^{(0)}$.

We assume a local tunneling into the substrate with an effective tunneling matrix element $\mathbf{t}$. At second-order we find the tunneling energy scale $\gamma = 2\pi\nu_s|\mathbf{t}|^2$, where ν_s is the density-of-states in the substrate. We largely focus on the regime $\Delta_s \gg \gamma$, such that the tunneling scale is less than the substrate gap (for a less restrictive treatment, see the appendix) and we may treat processes only in the Andreev channel.

Provided the substrate superconducting phase is not strongly fluctuating (the relevant energy and length scales over which the phase varies are the plasma frequency and the in-plane penetration depth of the substrate, respectively), we can model the proximity-induced superconducting gap in the sample by adding a term to the Hamiltonian (see the appendix for derivation),

$$H_{\text{prox}} = -\frac{1}{2}\gamma \sum_{\mathbf{p}} c_{-\mathbf{p}\downarrow}c_{\mathbf{p}\uparrow}\frac{\overline{\Delta_s}}{|\Delta_s|} + c_{\mathbf{p}\uparrow}^\dagger c_{-\mathbf{p}\downarrow}^\dagger \frac{\Delta_s}{|\Delta_s|}. \qquad (3)$$

In particular, this opens a minigap at the Fermi level for the electrons in the sample (in the Andreev regime $|\Delta_s| \gg \gamma$, the size of the minigap is $\gamma/2$) and the phase is referenced with respect to the substrate phase. We henceforth set this phase to be zero, such that the substrate gap is taken to be real and positive.

Since the proximity effect opens a gap on the Fermi surface of the sample, we expect the intrinsic d-wave pairing transition to be suppressed. Indeed, by solving the mean-field equations in the d-wave channel in the presence of the proximity gap (as described in the appendix), we find that there is a depression of the critical temperature to $T_d < T_d^{(0)}$, as shown in Fig. 3a. We broadly expect this to be the case so long as the order parameters are not able to hybridize in presence of the interface; if they are able to, then this analysis should be revised to include the linear coupling between the two order parameters, as in Ref. [14]. A rudimentary analysis of the gap equation for T_d in the proximity-induced case is carried out in the appendix; within the BCS regime, this can be seen to modify the low-energy density of states and therefore is independent of the cutoff, except through dependence on $T_d^{(0)}$, a low-energy parameter.
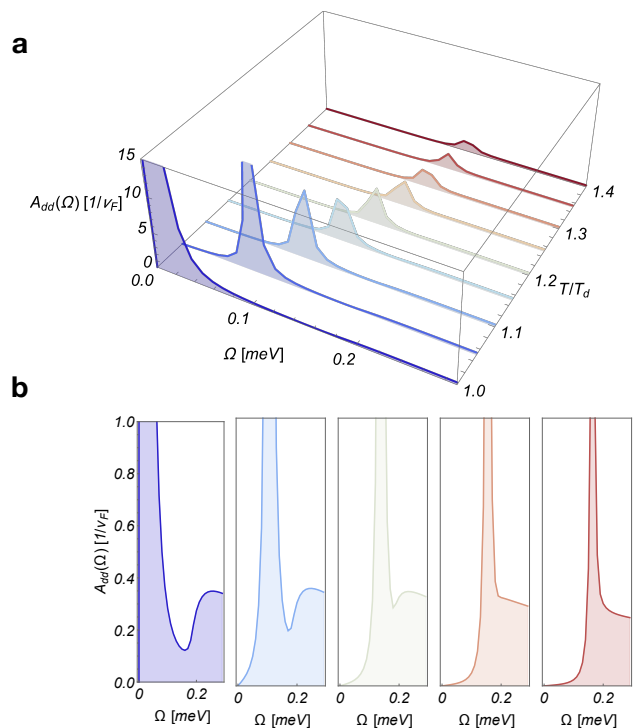
III. COLLECTIVE MODE

We now proceed to our main result: the emergence of the bound-state collective mode. Above the new d-wave transition temperature, the d-wave order is uncondensed but still fluctuates due to the remnant pairing interaction. Within the Random Phase Approximation we may derive an equation of motion which describes the dynamics of this fluctuating d-wave order. This is derived in detail in the appendix, but it may be understood as the linear-response pair-susceptibility of the sample in the proximitized state [32]. The presence of a bound-state collective mode then shows up as a resonance in the pair-susceptibility.

We separate the d-wave order parameter into the components which are in-phase and out-of-phase with respect to the substrate condensate, writing $\Delta_{\mathbf{q}}^d(t) = h_{\mathbf{q}}(t) + id_{\mathbf{q}}(t)$. We find that the in-phase component $h_{\mathbf{q}}$ has no sharp resonance and essentially mirrors the two-particle continuum, and thus we will henceforth neglect the in-phase component. This is in line with the expectation that the s- and d-wave orders are competing and therefore the "repulsion" between the two orders is minimized when they are mutually out of phase [9].

At linear order we calculate the spectral function for the dynamic pair-susceptibility in the out-of-phase fluctuation $d_{\mathbf{q}}$ channel

$$\mathcal{A}_{dd}(\Omega, \mathbf{q}) = -\frac{1}{\pi}\Im\left\{-i\int_0^\infty dt\, e^{i\Omega t}\langle [d_{\mathbf{q}}(t), d_{-\mathbf{q}}(0)]\rangle\right\},$$
(4)

which in particular captures the binding energy and linewidth of the d-wave excitation. The spectral func-

FIG. 2. Evolution of the collective mode spectral function with temperature. Panels (**a**) and (**b**) are different visualizations of the same function. (**a**) The collective mode spectral function for temperatures between T_d and $1.4\,T_d$, from which we see that the spectral peak of the mode sharpens and progressively softens as the temperature is lowered. At $T = T_d$, the mode ultimately softens to zero frequency. (**b**) Close-up depiction of the spectral function in (**a**) for $T/T_d = 1, 1.1, 1.2, 1.3, 1.4$. We see that the mode clearly separates from the quasiparticle continuum below $T \lesssim T_d^{(0)}$, and softens completely at T_d. In both we fix the tunneling strength $\gamma = .2$ meV and substrate gap to be $\Delta_s = 1.0$ meV, and hold the cutoff $\Lambda = 30$ meV and BCS constant $\lambda_d^{-1} = 4.58658$, corresponding to an intrinsic critical temperature of $T_d^{(0)} = .344$ meV. The finite γ leads to a reduced critical temperature of $T_d = .282$ meV, giving ratio $T_d^{(0)} \sim 1.2 T_d$.

tion $\mathcal{A}_{dd}(\Omega, \mathbf{q})$ is obtained in the appendix in terms of the Nambu-Gor'kov Green's functions using the Keldysh technique, although it may also be calculated using, e.g. the Anderson pseudo-spin method provided $|\Delta_s| \gg \gamma$, so that retardation and damping due to the substrate may be safely neglected.

We present the spectral function $\mathcal{A}_{dd}(\Omega, \mathbf{q} = 0)$ in Fig. 2 for different temperatures $T \geq T_d$ at fixed $\gamma, \Delta_s, T_d^{(0)}$. In Fig. 2(a) we show the evolution of the collective mode frequency and spectral weight with temperature. At high temperatures, we see no clear distinction between the collective mode and the bottom of the quasiparticle continuum. Lowering the temperature reduces the thermal broadening and pulls the mode out of the continuum, yielding a sharp collective mode which resides within the minigap. This is emphasized in Fig. 2(b), where we show the same spectral function, now focusing
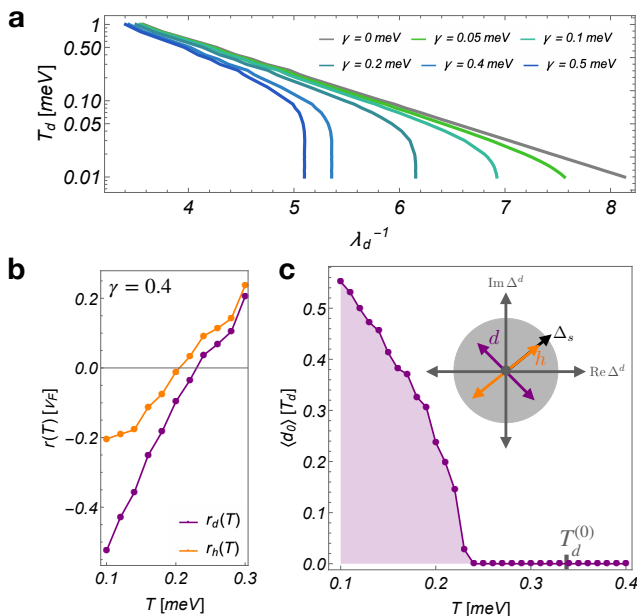
FIG. 3. (a) Transition temperature T_d of the sample as a function of the dimensionless d-wave coupling constant $\lambda_d = \nu_F g_d$, plotted for different values of the tunneling rate γ. Notice that for any fixed λ_d, T_d is suppressed as the tunneling rate is increased. (b) Temperature dependence of the quadratic coefficients in the Ginzburg-Landau expansion for h and d. The change of sign of each coefficient signals condensation in that channel, and one sees that the out-of-phase d mode condenses first. (c) Amplitude of the sample order parameter $\Delta^d = i\langle d \rangle$ near T_d. Inset: illustration of the relative Higgs and Bardasis-Schrieffer modes, and their phase relative to the s-wave substrate order parameter

on the relation between the collective mode and continuum. This separation occurs once the temperature $T \sim T_d^{(0)}$, the characteristic temperature scale of the intrinsic pairing interactions. As we decrease the temperature further the mode continues to soften. Qualitatively, we find that the sharp collective mode resides within the region of $T_d < T < T_d^{(0)}$, which makes sense given that it is a manifestation of the intrinsic pairing fluctuations, which in turn are relevant for $T \lesssim T_d^{(0)}$. In the appendix we show that to lowest order in the minigap γ, in the purely Andreev limit, the size of this regime roughly behaves as $(T_d - T_d^{(0)})/T_d^{(0)} \sim -\frac{7\zeta(3)\gamma^2}{32\pi^2(T_d^{(0)})^2}$, valid for small γ. Remarkably, at $T = T_d < T_d^{(0)}$ the mode softens completely, and we see the d-wave bound-state itself condenses. As we now demonstrate, this signals the onset of a second phase transition into a state with finite d-wave order.

IV. TIME-REVERSAL SYMMETRY BREAKING

In fact, this split transition behavior is generic to systems with strongly competing superconducting orders,

and in this case it signals the onset of time-reversal symmetry breaking [7–9]. This is understood by noting that the collective mode is in the out-of-phase channel, and therefore is odd under time-reversal symmetry. Condensing this mode requires spontaneously choosing the relative phase to be $\pm\pi/2$, entering into either an $s + id$ or $s - id$ state [8, 9].

This intuition is confirmed by explicitly solving the Ginzburg-Landau mean-field equation for the d-mode as we pass through the temperature T_d. Expanding the gap equation Eq. 2 for small Δ_d we obtain an equation for the static, homogeneous component of $d_{q=0} \equiv d$ (see appendix) of

$$\left(r_d + u_d d^2 \right) d = 0. \tag{5}$$

The coefficients $r_d \sim T - T_d$ and $u_d \sim 1/T^2$ [33], as well as the quadratic Ginzburg-Landau coefficient for the amplitude mode r_h are calculated microscopically in the appendix. In Fig. 3(b), we plot the coefficients r_d and r_h and see explicitly that r_d changes sign first at $T = T_d$, so that below T_d the order parameter d acquires a non-zero value shown explicitly in Fig. 3(c). Note this transition does not spontaneously break $U(1)$ symmetry, which has already been broken by the substrate order parameter, but it does break the remnant $\mathbb{Z}_2$ symmetry, under which $id \rightarrow -id$.

The breaking of time-reversal symmetry in such an "s-d" heterostructure has been predicted previously, for instance at the twin-grain boundaries in cuprate systems [34–36], at the interface of "s-d" superconductors [37–39], and between twisted cuprate layers [40–42]. Our calculation indicates that the breaking of time-reversal symmetry in these systems ought to be heralded by a softening collective mode, as we have shown. It is also worth commenting that, just as we have shown the Bardasis-Schrieffer collective mode emerges in the normal state of the heterostructure, we may also expect a new collective mode to emerge once time-reversal symmetry is broken below T_d [17, 21, 22, 24], thereby making connection to previous proposals for collective mode spectroscopy. This may also be relevant for multiband systems which break time-reversal symmetry due to frustrated interband couplings [10, 23, 43–45].

In the appendix, we explore the collective mode dependence on the substrate gap Δ_s and the minigap γ. To summarize, the coherent, sharp character of the collective mode is best when the substrate gap Δ_s and minigap γ are both large, while maintaining $\gamma \ll \Delta_s$. If the minigap γ is too small then the collective mode essentially becomes indistinguishable from the quasiparticle continuum [46]. Similarly, if the substrate gap Δ_s is too small, then the collective mode can overlap with the substrate continuum, in which case the substrate acts as an incoherent reservoir, destroying the collective mode. We then recover the known behavior for overdamped fluctuations of the sample's superconducting order [47], with the d-wave pairs decaying with a characteristic lifetime $\tau \sim 1/(T - T_d)$, thereby also allowing for the study of crit-

ical superconducting fluctuations [32, 48, 49]. As such, in order to apply this protocol, it is best to choose a substrate with as large a quasiparticle gap as possible, and to make good electrical contact with the sample, yielding the largest possible tunneling matrix element $\mathfrak{t}$.

In practice, this is an experimental challenge, since it requires a clean interface with strong coherent tunneling matrix element $\mathfrak{t}$ between the two materials. While the minigap $\gamma \sim |\mathfrak{t}|^2$ need not be large as compared to the substrate gap Δ_s, it does control the size of the temperature regime over which the mode exists and is sharp, with the relevant window scaling as $(\gamma/T_d^{(0)})^2$. Thus, it remains an experimental challenge as to whether it can be made large enough in such a heterostructure as to enable this kind of coherent mode. Nevertheless, recent advances in the assembly of two-dimensional materials offers some encouraging signs that this may be feasible [50–53].

V. EXPERIMENTAL PROSPECTS

Finally, we briefly discuss various experimental signatures of this mode. The first is electron tunneling spectroscopy [25–27, 54]. In inelastic tunneling spectroscopy, bosonic excitations such as phonons [55] and magnons [56] are routinely observed by studying characteristic $I - V$ curves. In particular, these bosonic excitations may appear as a sharp feature in d^2I/dV^2, which signals the opening of a new inelastic scattering channel for electrons at that bias energy. In this context, we may imagine it is also possible for an electron to emit a collective mode in the process of tunneling in to the sample, and therefore we should also expect a similar kink feature to appear in the $I - V$ curve once the energy passes the collective mode threshold. While this is still a relatively difficult measurement to perform, there is some precedent for using this technique to study collective modes of unconventional superconductors [57, 58]. Since, as we have seen, the collective mode we identify here can have strong temperature dependence, this may help to identify such a feature since it in principle will soften considerable as the temperature is lowered.

In a similar vein, it may also be possible to identify this collective mode using ARPES, in which case the mode will again manifest as an inelastic contribution to the electronic self-energy [59–61]. In this context, ARPES has the additional benefit of potentially observing the momentum dependence of the coupling, which could help identify the symmetry channel of the collective mode, and thus the symmetry of the underlying pairing interaction.

Lastly, we expect Raman spectroscopy to also be sensitive to the collective mode. This is not surprising since it is known that the Bardasis-Schrieffer mode, when it exists, is Raman active [62–64]. Like ARPES, Raman spectroscopy also has the potential to probe the selection rules of the collective mode in addition its frequency.

Finally, we discuss promising materials for the realization of this proposal. In our model, we considered

a d-wave system but this is not crucial; much of what we assumed only relied on the sample order parameter being orthogonal to the s-wave substrate order. However, we do want the intrinsic critical temperature $T_d^{(0)}$ to be low compared to the bulk transition temperature of the substrate, T_s. There are a number of interesting van der Waals compounds [65, 66], such as MoS_2 [67, 68], $NbSe_2$ [69], WS_2 [70], and WTe_2 [71–73] which exhibit possibly unconventional superconductivity and can be exfoliated into thin layers. Additionally, moiré bilayer and trilayer graphene likely exhibit unconventional superconductivity at a low temperature scale [74–77].

In this vein, we study one particular model of pairing in graphene, wherein it was proposed that magnetic fluctuations may be responsible for pairing, and that the preferred ground state is an intervalley f-wave triplet state [29]. In the appendix we consider proximity-inducing a gap in this system and carry out the calculation for the proximity-induced collective modes in this system. Within the quasiclassical approximation $\Delta/E_F \ll 1$, we find essentially no formal difference as compared to the case of d-wave pairing described in the text, except that due to the triplet nature of the pairing we predict there will be three degenerate collective modes—one for each of the spin components. This presents a possible route towards confirming this as the pairing in graphene, especially since in the presence of the spin degree of freedom these modes may also couple optically via magnetic dipole interactions, allowing for their identification via microwave ferromagnetic resonance spectroscopy [2].

It may also be possible to study this physics using a severely overdoped cuprate, provided the transition temperature can be depressed below that of a realistic s-wave system. This has the benefit of having an established gap-symmetry and therefore may offer a useful test-case. In addition, recent efforts have established that certain cuprates may also be prepared in thin layers, or even single copper-oxide layers [78]. In this context, our proposal has some technical overlap with recent proposals for time-reversal symmetry breaking chiral superconductivity in systems of twisted cuprate monolayers [40–42].

In addition to challenges concerning the quality of the interface, another limitation of our proposal is the requirement that the s-wave substrate superconductor have a higher critical temperature than the sample. There are relatively few choices which maximize the substrate transition temperature, with the most likely candidate substrates being Nb, NbN, or NbTiN, with $T_s \sim 7-15$ K. It may also be possible to use a fullerene such as Rb_3C_{60}, with $T_s \sim 30$K, at the expense of likely introducing other complications [79].

It would be interesting to try and apply our results to sample superconductors which already feature intrinsic collective modes but which are overdamped. By opening a proximity-induced gap, one may attempt to, e.g. stabilize the Higgs collective mode, which is usually located at the gap edge and subject to quasiparticle damping [80]. In

this way, much like a charge-density wave order parameter can separate the Higgs mode from the continuum and enable its coherent oscillation [81–83], it might also be possible to use the small proximity-induced gap to separate the continuum from the Higgs mode and enable its widespread detection.

In conclusion, we have considered a simple model of an unconventional superconducting sample that is proximitized by an s-wave superconducting substrate and shown that this can lead to a sharp collective mode which captures the intrinsic pairing interaction in the sample. This potentially greatly expands the platforms for studying unconventional superconductivity through their collective modes and increases the number of experimental probes amenable to these difficult-to-characterize states.

VI.   ACKNOWLEDGMENTS

Appendix A: Substrate Self-Energy

Here we derive the self-energy for the sample electrons and in particular recover the proximity effect Hamiltonian in the regime dominated purely by Andreev processes.

For a detailed treatment see, for instance, Ref. 84–86. We begin by employing the Matsubara framework and model the tunneling interaction via

$$\mathcal{S}_{\text{int}} = -\mathfrak{t} \int d^2r \int d\tau \left[\overline{\psi}(x)\tau_3 \Psi(x, z=0) + \overline{\Psi}(x, z=0)\tau_3 \psi(x) \right]. \tag{A1}$$

Here $\mathfrak{t}$ is an effective local, spin and momentum independent tunneling matrix element, and $\psi(x)$ is used to describe the electrons in the thin-layer sample while $\Psi(x, z)$ describes the electrons in the substrate with depth $z \leq 0$ (the interface is taken to be at $z = 0$).

We can formally integrate out the substrate electrons assuming a Gaussian approximation, which is well-justified if the phase fluctuations are frozen out. We then generate an effective action for the sample electrons of

$$\mathcal{S}_{\text{eff}} = -\log\langle e^{-S_{\text{int}}}\rangle \tag{A2}$$

with the expectation value evaluated using the substrate Green's function. We find the formal result

$$\mathcal{S}_{\text{eff}} = -\mathfrak{t}^2 \int d^3x d^3x' \overline{\psi}(x')\tau_3 \langle \Psi(x', z=0)\overline{\Psi}(x, z=0)\rangle \tau_3 \psi(x), \tag{A3}$$

or in terms of the substrate Green's function

$$\mathcal{S}_{\text{eff}} = \mathfrak{t}^2 \int d^3x d^3x' \overline{\psi}(x')\tau_3 \hat{\mathbb{G}}_{\text{sub}}(x', z=0; x, z=0)\tau_3 \psi(x). \tag{A4}$$

We use the well-known "local approximation" which evaluates the substrate Green's function locally in space via

$$\hat{\mathbb{G}}_{\text{sub}}(x', z=0; x, z=0) \sim \hat{\mathbb{G}}_{\text{sub}}(\tau', \mathbf{r}; \tau, \mathbf{r})\delta^2(\mathbf{r}' - \mathbf{r}). \tag{A5}$$

This is then related to the local density-of-states in the substrate in the frequency domain as

$$\hat{\mathbb{G}}_{\text{sub}}(i\varepsilon_m; \mathbf{r}, \mathbf{r}) = \int_{\mathbf{p}} (i\varepsilon_m - \xi_{\mathbf{p}}\tau_3 - \Delta_s\tau_1)^{-1} = -\pi\nu_s \frac{i\varepsilon_m + \Delta_s\tau_1}{\sqrt{\varepsilon_m^2 + \Delta_s^2}}. \tag{A6}$$

In the effective action for the sample, this means that we find a contribution from the substrate of

$$\mathcal{S}_{\text{eff}} = \sum_p \overline{\psi}_p \mathbf{\Sigma}_s(p) \psi_p \tag{A7}$$

with self-energy

$$\mathbf{\Sigma}_s(p) = \mathfrak{t}^2 \tau_3 \hat{\mathbb{G}}_{\text{sub}}(i\varepsilon; \mathbf{r}, \mathbf{r}) \tau_3 = -\pi \nu_s \mathfrak{t}^2 \tau_3 \frac{i\varepsilon_m + \Delta_s \tau_1}{\sqrt{\varepsilon_m^2 + \Delta_s^2}} \tau_3 \equiv -\frac{\gamma}{2} \frac{i\varepsilon_m - \Delta_s \tau_1}{\sqrt{\varepsilon_m^2 + \Delta_s^2}}. \tag{A8}$$

This defines the tunneling scale as

$$\gamma = 2\pi \nu_s |\mathfrak{t}|^2. \tag{A9}$$

It is common to characterize the effect of the substrate in terms of the quasiparticle and gap renormalizations via

$$Z(i\varepsilon_m) = 1 + \frac{\gamma}{2} \frac{1}{\sqrt{\varepsilon_m^2 + \Delta_s^2}} \tag{A10a}$$

$$\Phi(i\varepsilon_m) = \frac{\gamma}{2} \frac{\Delta_s}{\sqrt{\varepsilon_m^2 + \Delta_s^2}}, \tag{A10b}$$

such that the electronic Green's function in the normal state of the sample is

$$\hat{\mathbb{G}}_{\text{sample}}^{-1}(i\varepsilon_m, \mathbf{p}) = Z(i\varepsilon_m)i\varepsilon_m - \xi_{\mathbf{p}}\tau_3 - \Phi(i\varepsilon_m)\tau_1. \tag{A11}$$

We can also analytically continue this result to get the retarded self-energy via

$$Z_R(\varepsilon) = 1 + \frac{\gamma}{2} \frac{1}{\sqrt{\Delta_s^2 - (\varepsilon + i0^+)^2}} \tag{A12a}$$

$$\Phi_R(\varepsilon) = \frac{\gamma}{2} \frac{\Delta_s}{\sqrt{\Delta_s^2 - (\varepsilon + i0^+)^2}}. \tag{A12b}$$

We note that in the limit of $\Delta_s \to \infty$ the quasiparticle renormalization becomes trivial and the anomalous term becomes the minigap, such that

$$Z_R(\varepsilon) \to 1 \tag{A13a}$$

$$\Phi_R(\varepsilon) \to \frac{\gamma}{2}\tau_1. \tag{A13b}$$

This justifies the use of a BdG Hamiltonian in this regime, dominated by the Andreev reflection back in to the sample, with proximity induced gap term.

Appendix B: Gap Equation

In this section, we discuss the mean-field properties of our model in the Matsubara imaginary time formalism. In particular, we solve the gap equation determining the transition temperature of the sample, T_d, and show that the resulting state of the coupled sample-substrate system spontaneously breaks time-reversal symmetry, with the sample order parameter condensing $\pi/2$ out-of-phase with the substrate order parameter, forming an $s + id$ state.

Taking into account the self-energy contribution from the coupling to the substrate, the Matsubara action for the sample reads

$$S = \frac{1}{g_d} \sum_q \bar{\Delta}_q^d \Delta_q^d - \text{tr} \log \mathbb{G}^{-1}, \tag{B1}$$

where Δ_q^d is the d-wave order parameter in the sample and the inverse Gor'kov Green function is

$$\hat{\mathbb{G}}^{-1}(p, q) = Z_n i\omega_n - \xi_{\mathbf{p}}\tau_3 - (\Phi_n + \Delta_q^d \chi_{\mathbf{p}}^d)\tau^{\dagger} + \text{h.c.} \tag{B2}$$

where $\omega_n = 2\pi(n + \frac{1}{2})T$ is a fermionic Matsubara frequency and τ_i are the Pauli matrices in Nambu space, with $\tau = \frac{1}{2}(\tau_1 - i\tau_2)$. The quasiparticle renormalization and anomalous self energy due to the substrate are

$$Z_n = 1 + \frac{\gamma}{2} \frac{1}{\sqrt{\omega_n^2 + \Delta_s^2}} \tag{B3}$$

$$\Phi_n = -\frac{\gamma}{2} \frac{\Delta_s}{\sqrt{\omega_n^2 + \Delta_s^2}} . \tag{B4}$$

The BCS gap equation for the homogeneous order parameter $\Delta^d \equiv \Delta_{q=0}^d$ is given by the saddle point of this action,

$$\Delta^d = -g_d T \sum_p \chi_{\mathbf{p}}^d \, \mathrm{tr}\, \hat{\mathbb{G}}(p,0)\tau = g_d T \sum_p \chi_{\mathbf{p}}^d \frac{\Delta^d \chi_{\mathbf{p}}^d + \Phi_n}{Z_n^2 \omega_n^2 + \Phi_n^2 + |\Delta^d|^2 \left(\chi_{\mathbf{p}}^d\right)^2} . \tag{B5}$$

The critical temperature T_d of the sample can be determined by solving the gap equation in the limit $\Delta_d \to 0$. In this limit, the gap equation reduces to

$$\lambda_d^{-1} = 2\pi T_d \sum_{\omega_n < \Lambda} \frac{1}{\sqrt{Z_n^2 \omega_n^2 + \Phi_n^2}} = 2\pi T_d \sum_{\omega_n < \Lambda} \left[\left(1 + \frac{\gamma}{\sqrt{\omega_n^2 + \Delta_s^2}}\right) \omega_n^2 + \frac{\gamma^2}{4} \right]^{-1/2} , \tag{B6}$$

where $\lambda_d = \nu_F g_d$ is the dimensionless d-wave coupling constant (with ν_F the density of states at the Fermi level) and we have written $\sum_p = \nu_F \sum_{\omega_n} \int \mathrm{d}\xi \int \frac{\mathrm{d}\theta_{\mathbf{p}}}{2\pi}$ and performed the integrals over $\theta_{\mathbf{p}}$ and ξ. The frequency cutoff Λ can be expressed in terms of a dimensionless cutoff N on the Matsubara index as $\Lambda = 2\pi N T_d$.

We can approach the problem from a complementary perspective by expanding the action (B1) in powers of Δ^d, which furnishes an effective Ginzburg-Landau theory, valid near T_d. As discussed in the main text, it is useful to decompose Δ^d into its components in-phase and out-of-phase with the substrate order parameter, writing $\Delta^d = h + id$. In this section, we will be concerned with only the static, homogeneous order parameter at the level of mean field theory, and thus neglect the frequency and momentum dependence of the fields h and d.

To organize the expansion, we write the Gor'kov Green function as $\hat{\mathbb{G}}^{-1} = \hat{\mathbb{G}}_0^{-1} + \hat{\Lambda}^h h + \hat{\Lambda}^d d$, with $\hat{\Lambda}^h = -\chi_{\mathbf{p}}^d \tau_1$ and $\hat{\Lambda}^d = \chi_{\mathbf{p}}^d \tau_2$. Expanding (B1) to fourth order in h and d, we find

$$S = r_h h^2 + r_d d^2 + u_h h^4 + u_d d^4 + u' d^2 h^2 . \tag{B7}$$

The superconducting transition occurs when r_d or r_h changes sign, signalling an instability in the in-phase (nematic) or out-of-phase (time reversal symmetry breaking) channel. Both of these functions are related to the (inverse) fluctuation propagator $L_{dd}^{-1}(q = 0)$ discussed in the main text, and are explicitly given by

$$r_h(T) = g_d^{-1} + \frac{T}{2} \sum_p \left(\chi_{\mathbf{p}}^d\right)^2 \mathrm{tr}\left(\hat{\mathbb{G}}_0 \hat{\Lambda}^h\right)^2 = g_d^{-1} - 2\pi\nu T \sum_{\omega_n < \Lambda} \frac{1}{\sqrt{Z_n^2 \omega_n^2 + \Phi_n^2}} + \pi\nu T \sum_{\omega_n < \Lambda} \frac{\Phi_n^2}{[Z_n^2 \omega_n^2 + \Phi_n^2]^{3/2}} \tag{B8}$$

$$r_d(T) = g_d^{-1} + \frac{T}{2} \sum_p \left(\chi_{\mathbf{p}}^d\right)^2 \mathrm{tr}\left(\hat{\mathbb{G}}_0 \hat{\Lambda}^d\right)^2 = g_d^{-1} - 2\pi\nu T \sum_{\omega_n < \Lambda} \frac{1}{\sqrt{Z_n^2 \omega_n^2 + \Phi_n^2}} . \tag{B9}$$

Clearly, the zeroes of $r_d(T)$ coincide with the solutions to (B6) which determine T_d. Moreover, one finds numerically that the second term in r_h above is always positive, so that r_d always changes sign first (i.e., before r_h) as the temperature is lowered. This implies that the sample order parameter condenses out-of-phase with the substrate order parameter, $\Delta^d \sim id$ which implies the system spontanously breaks time reversal symmetry at T_d.

To stabilize the expansion in d, we must calculate the quartic coefficient u_d, which is given by

$$u_d = \frac{3\nu}{8} 2\pi T \sum_{\omega_n < \Lambda} \frac{1}{[Z_n^2 \omega_n^2 + \Phi_n^2]^{3/2}} . \tag{B10}$$

We may then solve the saddle point equation for d, as discussed in the main text, which allows us to determine the equilibrium value of the sample order parameter near T_d,

$$\langle \Delta^d \rangle = i\langle d \rangle = i\sqrt{\frac{-r_d(T)}{2u_d}} . \tag{B11}$$

Appendix C: Dependence of Transition Temperature on Parameters

Here we analyze in more detail the dependence of the transition temperature reduction on parameters like the cutoff. The transition temperature T_d is determined by solving the linearized gap equation. In Matsubara frequency this reads

$$\lambda_d^{-1} = 2\pi T_d \sum_{\omega_n < \Lambda} \frac{1}{\sqrt{Z_n^2 \omega_n^2 + \Phi_n^2}} = 2\pi T_d \sum_{\omega_n < \Lambda} \left[\left(1 + \frac{\gamma}{\sqrt{\omega_n^2 + \Delta_s^2}}\right) \omega_n^2 + \frac{\gamma^2}{4} \right]^{-1/2}. \tag{C1}$$

We are interested in how this compares to the bare transition temperature, which is found by solving this equation when $\gamma = 0$. We note that in the regime considered in this paper, $\Lambda \gg \Delta_s$, and that the leading divergence is still the logarithmic Cooper divergence steming from the summation over frequencies $\Delta_s < \omega_n < \Lambda$, giving $\log(\Lambda)$. We therefore subtract off this leading divergence, which can then be evaluated in terms of $T_d^{(0)}$ to get

$$\lambda_d^{-1} = 2\pi T_d \sum_{\omega_n < \Lambda} \frac{1}{|\omega_n|} + \frac{1}{\sqrt{Z_n^2 \omega_n^2 + \Phi_n^2}} - \frac{1}{|\omega_n|} = \log\left(\frac{2\Lambda e^{\gamma_E}}{\pi T_d}\right) + 2\pi T_d \sum_{\omega_n} \frac{1}{\sqrt{Z_n^2 \omega_n^2 + \Phi_n^2}} - \frac{1}{|\omega_n|}. \tag{C2}$$

Now, the remaining summation is finite and therefore does not depend on the cutoff Λ, implying that the only dependence of $T_d/T_d^{(0)}$ comes indirectly through the coupling constant and bare transition $T_d^{(0)}$.

Specifically, we find

$$\log\left(\frac{T_d}{T_d^{(0)}}\right) = 2\pi T_d \sum_{\omega_n} \frac{1}{\sqrt{\omega_n^2 (1 + \frac{\gamma}{\sqrt{\omega_n^2 + \Delta_s^2}}) + \gamma^2/4}} - \frac{1}{|\omega_n|}. \tag{C3}$$

The right hand side clearly vanishes as $\gamma \to 0$, in which case this implies $T_d \to T_d^{(0)}$. We now more closely consider the regime where $\gamma \ll T_d \ll \Delta_s$, corresponding to a small minigap but large substrate gap. In this case, we can safely approximate the sum by

$$\log\left(\frac{T_d}{T_d^{(0)}}\right) \sim 2\pi T_d \sum_n \left[\frac{1}{\sqrt{\omega_n^2 + \frac{\gamma^2}{4}}} - \frac{1}{\omega_n} \right]. \tag{C4}$$

We study this by expanding in small γ/T_d. We find corrected gap equation

$$\log\left(\frac{T_d}{T_d^{(0)}}\right) \sim -\frac{\gamma^2}{4} \frac{\pi T_d}{(2\pi T_d)^3} \sum_{n=0}^{\infty} \frac{1}{(n + \frac{1}{2})^3} = -\frac{7\zeta(3)\gamma^2}{32\pi^2 T_d^2}. \tag{C5}$$

This is solved by using the Lambert W function $W_0(x)$, such that

$$T_d/T_d^{(0)} = \sqrt{-\frac{7\zeta(3)\gamma^2}{32\pi^2 (T_d^{(0)})^2 W_0\left(-\frac{7\zeta(3)\gamma^2}{32\pi^2 (T_d^{(0)})^2}\right)}}. \tag{C6}$$

Note that for small x, $W_0(x) \sim x$ so that as $\gamma \to 0$ we recover $T_d = T_d^{(0)}$. This is plotted in Fig. 4. For small γ we find

$$T_d/T_d^{(0)} = \frac{1}{\sqrt{1 + \frac{7\zeta(3)\gamma^2}{32\pi^2 (T_d^{(0)})^2}}}. \tag{C7}$$

In Fig. 5, we compare this analytical estimate against the explicit numerical solution for different parameters. In the left-side panel of Fig. 5, we consider the same parameters as used in the main text, in which case the Δ_s is not particularly large. We see that the analytical estimate is fairly poor quantitatively in this case, although it does serve as an upper bound, indicating that the departures from the simple estimate in fact make the effect larger than predicted. On the right-side panel, we use an artificially large value of Δ_s (while still taking it less than the cutoff in most cases) and find that this improves agreement with the analytical estimate. Overall, we therefore conclude that the analytical estimate obtained here is qualitatively useful, and shows how the relevant energy scales enter, but it tends to underestimate the actual importance of the effects we outline in this paper.
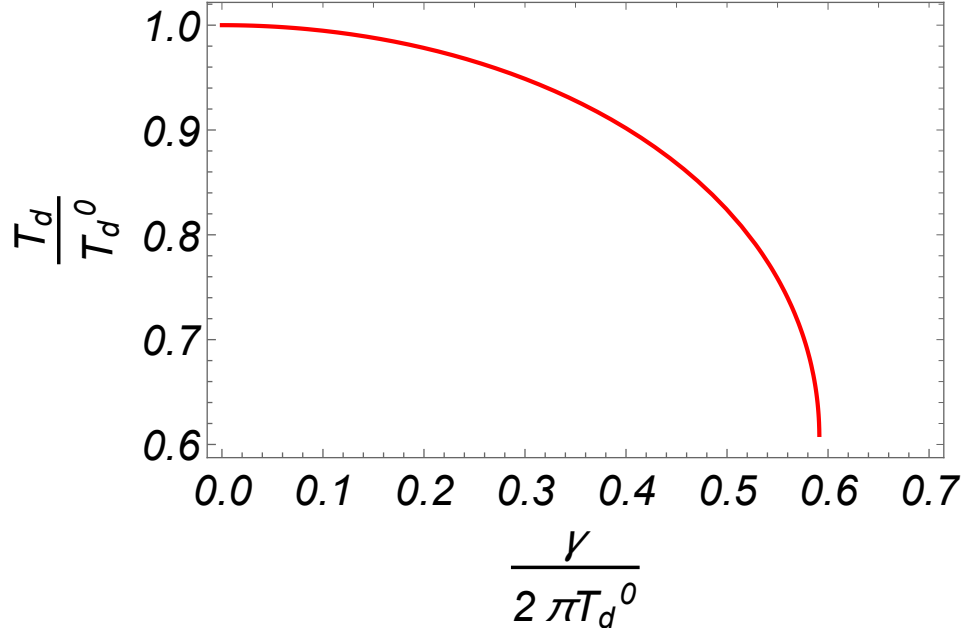
FIG. 4. Analytical estimate for the depressed critical temperature as a function of minigap following the functional form of Eqn. C6, derived under assumption $\Delta_s \to \infty$. Here we plot for rather large values of γ to illustrate the full dependence, however we note that once $\gamma \sim \pi T_d$ the solution presented begins to lose validity.
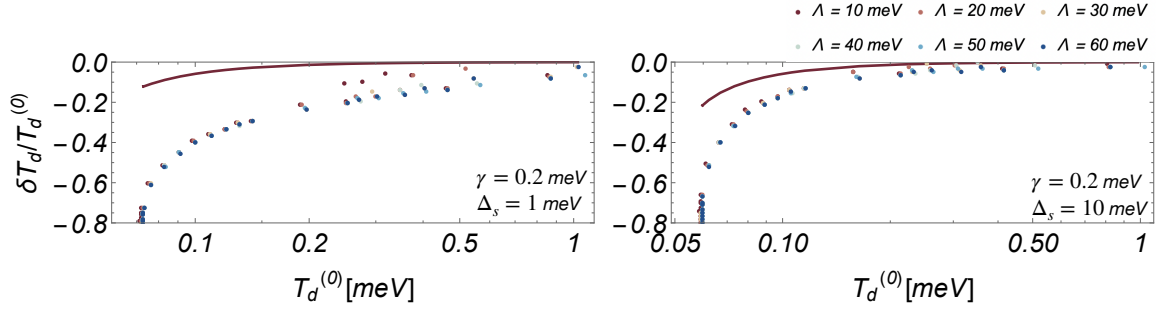
FIG. 5. Comparison of the analytical estimate Eq. C6 for T_d to numerical solutions for varying values of the cutoff Λ. In the left panel, we study $\delta T_d \equiv T_d - T_d^{(0)}$ for the parameters used in the main text, but where the analytical estimate Eq. C6 is not well-justified. In the right panel, we consider a case where Eq. C6 is better justified. We find this analytical estimate agrees with the numerical results for $T_d^{(0)} \gtrsim \gamma$. Notably, the numerical results are not explicitly dependent on the cutoff, and depend only on the cutoff through $T_d^{(0)}$.

Appendix D: Collective Mode Propagator

Here we derive the collective mode propagators in the Random Phase Approximation using the Keldysh technique.

We follow Kamenev [87] and introduce fermion fields on the $\pm$ time contours. The BCS action can be written in terms of Nambu-Gorkov space for each time-contour as

$$
S = \int dt \sum_{\mathbf{p}} \overline{\psi}_{\mathbf{p}} \sigma_3 \left[i\partial_t - \xi_{\mathbf{p}} \tau_3 \right] \psi_{\mathbf{p}}
$$

$$
+ g_d \sum_{\mathbf{q}} \int_{\mathbf{p},\mathbf{p}'} \chi^d_{\mathbf{p}} \chi^d_{\mathbf{p}'} \int dt \left[\overline{\psi}_{\mathbf{p}+\frac{1}{2}\mathbf{q}+} \tau^\dagger \psi_{\mathbf{p}-\frac{1}{2}\mathbf{q}+} \overline{\psi}_{\mathbf{p}'-\frac{1}{2}\mathbf{q}+} \tau \psi_{\mathbf{p}'+\frac{1}{2}\mathbf{q}+} - \overline{\psi}_{\mathbf{p}+\frac{1}{2}\mathbf{q}-} \tau^\dagger \psi_{\mathbf{p}-\frac{1}{2}\mathbf{q}-} \overline{\psi}_{\mathbf{p}'-\frac{1}{2}\mathbf{q}-} \tau \psi_{\mathbf{p}'+\frac{1}{2}\mathbf{q}-} \right] \quad \text{(D1)}
$$

Here τ are the Nambu-Gor'kov matrices and σ are the Keldysh matrices. We perform the Larkin-Ovchinikov rotation

$$\begin{pmatrix} \psi_{\mathbf{p}+} \\ \psi_{\mathbf{p}-} \end{pmatrix} = \frac{1}{\sqrt{2}}(\sigma_1 + \sigma_3) \begin{pmatrix} \psi_{\mathbf{p}S} \\ \psi_{\mathbf{p}A} \end{pmatrix}, \quad (\overline{\psi}_{\mathbf{p}+}, \overline{\psi}_{\mathbf{p}-}) = (\overline{\psi}_{\mathbf{p}S}, \overline{\psi}_{\mathbf{p}A}) \frac{1}{\sqrt{2}}(\sigma_1 + \sigma_3)\sigma_3. \tag{D2}$$

We henceforth use ψ to indicate the rotated spinor. The action is

$$S = \int dt \sum_{\mathbf{p}} \overline{\psi}_{\mathbf{p}} \left[i\partial_t - \xi_{\mathbf{p}}\tau_3\right] \psi_{\mathbf{p}}$$
$$+ g_d \sum_{\mathbf{q}} \int_{\mathbf{p},\mathbf{p}'} \chi_{\mathbf{p}}^d \chi_{\mathbf{p}'}^d \int dt \left[\overline{\psi}_{\mathbf{p}+\frac{1}{2}\mathbf{q}} \frac{\sigma_1}{2}\tau^\dagger \psi_{\mathbf{p}-\frac{1}{2}\mathbf{q}} \overline{\psi}_{\mathbf{p}'-\frac{1}{2}\mathbf{q}}\tau\psi_{\mathbf{p}'+\frac{1}{2}\mathbf{q}} + \overline{\psi}_{\mathbf{p}+\frac{1}{2}\mathbf{q}}\tau^\dagger\psi_{\mathbf{p}-\frac{1}{2}\mathbf{q}}\overline{\psi}_{\mathbf{p}'-\frac{1}{2}\mathbf{q}}\frac{\sigma_1}{2}\tau\psi_{\mathbf{p}'+\frac{1}{2}\mathbf{q}}\right]. \tag{D3}$$

We perform a Hubbard-Stratonovich decoupling of the interaction in the Cooper channel. Introducing fields $\Delta_{\mathbf{q}}^{cl}(t), \Delta_{\mathbf{q}}^q(t)$ and their conjugates the action can be recast as

$$S = \int dt \sum_{\mathbf{p}} \overline{\psi}_{\mathbf{p}} \left[i\partial_t - \xi_{\mathbf{p}}\tau_3\right] \psi_{\mathbf{p}}$$
$$- \sum_{\mathbf{q}} \int_{\mathbf{p}} \int dt \left[\overline{\psi}_{\mathbf{p}-\frac{1}{2}\mathbf{q}}\chi_{\mathbf{p}}^d \overline{\Delta}_{\mathbf{q}}^{cl}\tau\psi_{\mathbf{p}+\frac{1}{2}\mathbf{q}} + \overline{\psi}_{\mathbf{p}+\frac{1}{2}\mathbf{q}}\chi_{\mathbf{p}}^d \Delta_{\mathbf{q}}^{cl}\tau^\dagger\psi_{\mathbf{p}-\frac{1}{2}\mathbf{q}}\right]$$
$$+ \int dt \sum_{\mathbf{q}} \int_{\mathbf{p}} \overline{\Delta}_{\mathbf{q}}^q \left[\frac{-1}{g_d}\Delta_{\mathbf{q}}^{cl} - \int_{\mathbf{p}} \chi_{\mathbf{p}}^d \overline{\psi}_{\mathbf{p}-\frac{1}{2}\mathbf{q}}\frac{\sigma_1}{2}\tau\psi_{\mathbf{p}+\frac{1}{2}\mathbf{q}}+\right] + \Delta_{\mathbf{q}}^q \left[\frac{-1}{g_d}\overline{\Delta}_{\mathbf{q}}^{cl} - \int_{\mathbf{p}} \chi_{\mathbf{p}}^d \overline{\psi}_{\mathbf{p}+\frac{1}{2}\mathbf{q}}\frac{\sigma_1}{2}\tau^\dagger\psi_{\mathbf{p}-\frac{1}{2}\mathbf{q}}\right]. \tag{D4}$$

Here we see the field Δ^q acts a Lagrange multiplier for the classical field.
We simplify to get

$$S = \int dt \int_{\mathbf{p}} \sum_{\mathbf{q}} \overline{\psi}_{\mathbf{p}+\frac{1}{2}\mathbf{q}} \left[\delta_{\mathbf{q},0}(i\partial_t - \xi_{\mathbf{p}}\tau_3) - \tau^\dagger\chi_{\mathbf{p}}^d(\frac{\sigma_1}{2}\Delta_{\mathbf{q}}^q + \Delta_{\mathbf{q}}^{cl}) - \tau\chi_{\mathbf{p}}^d(\frac{\sigma_1}{2}\overline{\Delta}_{-\mathbf{q}}^q + \overline{\Delta}_{-\mathbf{q}}^{cl})\right]\psi_{\mathbf{p}-\frac{1}{2}\mathbf{q}} - \sum_{\mathbf{q}} \int dt \frac{1}{g_d}\left(\overline{\Delta}_{\mathbf{q}}^q\Delta_{\mathbf{q}}^{cl} + \overline{\Delta}_{\mathbf{q}}^{cl}\Delta_{\mathbf{q}}^q\right). \tag{D5}$$

This can be written compactly by introducing the Keldysh kernel

$$\check{\mathbb{G}}_{p,q}^{-1} = \delta_{q,0}(\varepsilon - \xi_{\mathbf{p}}\tau_3) - \chi_{\mathbf{p}}^d\left(\tau^\dagger\check{\Delta}_q + \tau\check{\overline{\Delta}}_{-q}\right) \tag{D6}$$

with the pair scattering vertices

$$\check{\Delta}_q = \frac{\sigma_1}{2}\Delta_q^q + \Delta_q^{cl}. \tag{D7}$$

Here, and throughout we indicate fermionic and bosonic four-momenta as $p = (\varepsilon, \mathbf{p}), q = (\omega, \mathbf{q})$.
We can now include the effect of the substrate via the retarded self-energy computed above. We have

$$\hat{\mathbf{\Sigma}}^R(\varepsilon) = -\frac{\gamma}{2}\left(\frac{\varepsilon - \Delta_s\tau_1}{\sqrt{\Delta_s^2 - (\varepsilon + i0^+)^2}}\right). \tag{D8}$$

From this we obtain the advanced self-energy as

$$\hat{\mathbf{\Sigma}}^A(\varepsilon) = -\frac{\gamma}{2}\left(\frac{\varepsilon - \Delta_s\tau_1}{\sqrt{\Delta_s^2 - (\varepsilon - i0^+)^2}}\right), \tag{D9}$$

and Keldysh self-energy via fluctuation-dissipation relation of

$$\hat{\mathbf{\Sigma}}^K(\varepsilon) = F(\varepsilon)\left(\hat{\mathbf{\Sigma}}^R(\varepsilon) - \hat{\mathbf{\Sigma}}^A(\varepsilon)\right). \tag{D10}$$

The function $F(\varepsilon)$ is the Keldysh occupation function and in equilibrium it is fixed to be

$$F(\varepsilon) = \tanh(\frac{\beta\varepsilon}{2}). \tag{D11}$$

This yields the Keldysh kernel of

$$\check{\mathbb{G}}_{p,q}^{-1} = \delta_{q,0} \left(\varepsilon - \xi_{\mathbf{p}} \tau_3 - \check{\boldsymbol{\Sigma}}(p) \right) - \chi_{\mathbf{p}}^d \left(\tau^\dagger \check{\Delta}_q + \tau \check{\overline{\Delta}}_{-q} \right), \tag{D12}$$

such that the BCS action is

$$S = -\frac{1}{g_d} \sum_q \left(\overline{\Delta}_q^q \Delta_q^{cl} + \overline{\Delta}_q^{cl} \Delta_q^q \right) + \overline{\psi} \cdot \check{\mathbb{G}} \cdot \psi, \tag{D13}$$

and the effective action obtained by integrating out the electrons is

$$S^{\text{eff}} = -\frac{1}{g_d} \sum_q \left(\overline{\Delta}_q^q \Delta_q^{cl} + \overline{\Delta}_q^{cl} \Delta_q^q \right) - i \mathbf{Tr} \log \check{\mathbb{G}}^{-1}[\Delta, \overline{\Delta}]. \tag{D14}$$

This functional of the order parameter is then evaluated in a saddle-point expansion.

1. Saddle-Point

For the saddle-point we take

$$\frac{\delta S^{\text{eff}}}{\delta \overline{\Delta}_q^q} = 0 \tag{D15}$$

and assume Δ_q^{cl} only has a condensate at zero momentum. We find the gap equation

$$-\frac{1}{g_d} \Delta^{cl} - i \int_p \text{tr} \check{\mathbb{G}}(p) (-\frac{\sigma_1}{2}) \tau \chi_{\mathbf{p}}^d = 0.$$

This reads

$$\frac{1}{g_d} \Delta^{cl} = \frac{i}{2} \int_p \text{tr} \chi_{\mathbf{p}}^d \tau \sigma_1 \check{\mathbb{G}}(p). \tag{D16}$$

The trace over the Keldysh space matrices gives the Keldysh component, such that

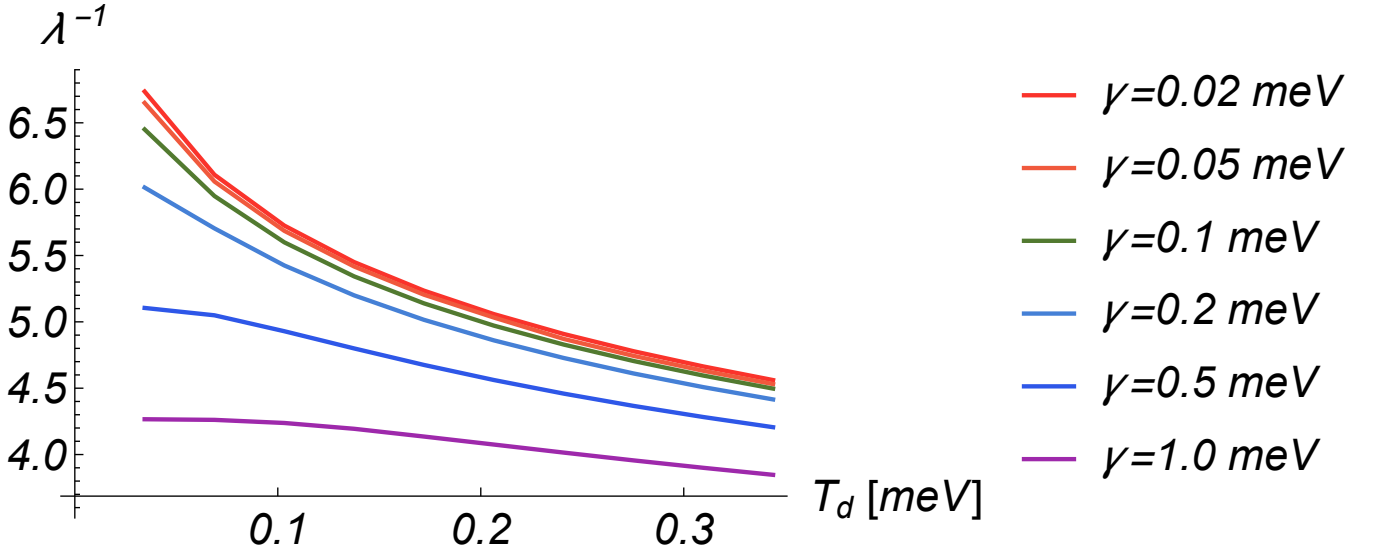$$\frac{1}{g_d} \Delta^{cl} = \frac{i}{2} \int_p \text{tr} \chi_{\mathbf{p}}^d \tau \hat{G}^K(p). \tag{D17}$$

We have

$$\hat{\mathbb{G}}^R(p) = \left(Z_R(\epsilon)\epsilon - \xi_{\mathbf{p}} \tau_3 - \Phi_R(\varepsilon)\tau_1 - \Delta^{cl} \chi_{\mathbf{p}}^d \tau^\dagger - \overline{\Delta}^{cl} \chi_{\mathbf{p}}^d \tau \right)^{-1} \tag{D18}$$

with the wavefunction renormalization and anomalous self-energy

$$Z_R = 1 + \frac{1}{2} \gamma \frac{1}{\sqrt{\Delta_s^2 - (\epsilon + i0^+)^2}}$$
$$\Phi_R(\varepsilon) = \frac{1}{2} \gamma \frac{\Delta_s}{\sqrt{\Delta_s^2 - (\epsilon + i0^+)^2}}. \tag{D19}$$

The trace over τ selects the anomalous component, while the integral over the d-wave form factor projects out the substrate contribution. Crucially, this only holds if the unconventional order is in an orthogonal channel to the s-wave substrate order. In the limit of small Δ^{cl}, using the fluctuation dissipation representation for $\check{\mathbb{G}}^K$ we find the linearized gap equation

$$\frac{1}{g_d} \Delta^{cl} = \frac{i}{2} \int_p F(\varepsilon)(\chi_{\mathbf{p}}^d)^2 \Delta^{cl} \left[\frac{1}{(Z_R(\varepsilon)\varepsilon)^2 - \xi_{\mathbf{p}}^2 - (\Phi_R(\varepsilon))^2} - \frac{1}{(Z_A(\varepsilon)\varepsilon)^2 - \xi_{\mathbf{p}}^2 - (\Phi_A(\varepsilon))^2} \right]. \tag{D20}$$

FIG. 6. Relationship between λ_d^{-1} and transition temperature T_d evaluated including the proximity-induced self-energy. Results are plotted for cutoff $\Lambda = 30$meV and substrate gap $\Delta_s = 1.057$meV, corresponding to a substrate transition temperature of $T_s = 7$K. We plot using causal regulator $0^+ = .005$meV and plot for a series of different tunneling size γ's, as indicated.

We make the quasiclassical approximation and average over the Fermi surface, enabled by the fact that the gap is s-wave and respects the symmetry of the Fermi surface. Introducing density-of-states at the Fermi level ν_F, and pairing constant $\lambda = g_d \nu_F$ we find

$$\frac{1}{\lambda} = \int d\varepsilon \frac{1}{2} \tanh \frac{\beta \varepsilon}{2} \int d\xi P(\varepsilon, \xi). \tag{D21}$$

with pairing spectral function

$$P(\varepsilon, \xi) = -\frac{1}{\pi} \Im \left[\frac{1}{(Z_R(\varepsilon)\varepsilon)^2 - \xi^2 - (\Phi_R(\varepsilon))^2} \right]. \tag{D22}$$

It is easily seen that this is an even function of ξ, which is cutoff at $\xi = \Lambda$, and we can see that $\varepsilon \to -\varepsilon$ corresponds to taking the complex conjugate (or alternatively, switches the R and A components), such that this is an odd function of ε. We therefore fold the integrations twice, noting tanh is also odd in ε. Thus we get

$$\frac{1}{\lambda} = 2 \int_0^\infty d\varepsilon \tanh \frac{\beta \varepsilon}{2} \int_0^\Lambda d\xi P(\varepsilon, \xi). \tag{D23}$$

Note that in the absence of the self-energy we have

$$P(\varepsilon, \xi) = \mathrm{sgn}(\varepsilon) \delta(\varepsilon^2 - \xi^2),$$

which gives the equation for λ of

$$\frac{1}{\lambda} = 2 \int_0^\Lambda d\xi \frac{\tanh(\beta \xi/2)}{2\xi} \Rightarrow T_d^{(0)} = \frac{2e^{\gamma_E}}{\pi} \Lambda e^{-1/\lambda},$$

which is the standard BCS gap equation. Here we have introduced the value of $T_d^{(0)}$ which is the intrinsic d-wave transition temperature in the absence of the substrate. In the presence of the substrate, this will be evaluated numerically.

This is complicated by the need to regularize the spectral functions with a factor of 0^+, and also to cutoff the integrals over ω at a finite high-frequency cutoff, which we take to be $\omega^* = 100$meV (the integrands decay rapidly in frequencies above the cutoff Λ). Throughout this we take $0^+ = .005$meV. All in all, we find the results including the proximity effect summarized in Fig. 6.

2. Collective Mode

We now consider the fluctuation propagator by expanding around the saddle-point. In the normal state with $\Delta^{cl} = 0$ we can expand to quadratic order in $\check{\Delta}$ to obtain the collective mode. In addition to the Hubbard-Stratonovich term, which is already quadratic in Δ, we also have to evaluate the functional determinant. Expanding this gives

$$\mathcal{S}_{\text{eff}} = -\frac{1}{g_d} \sum_q \left(\overline{\Delta}_q^{cl} \Delta_q^q + \overline{\Delta}_q^q \Delta_q^{cl} \right) + i\frac{1}{2} \mathbf{Tr} \check{\mathbb{G}}_0 \check{\Lambda} \check{\mathbb{G}}_0 \check{\Lambda}. \tag{D24}$$

We can simplify the calculation by first invoking the fluctuation dissipation relation, such that we only need to calculate the retarded propagator, which is the $cl - q$ component.

Furthermore, we decompose the d-wave mode in to the real and imaginary parts with respect to the substrate gap (which we take to be real). If we write

$$\Delta_q^\alpha = h_q^\alpha + id_q^\alpha \tag{D25}$$

for $\alpha = q, cl$ we then can write the pairing vertex as

$$\tau^\dagger \check{\Delta}_q + \tau \check{\overline{\Delta}}_{-q} = \sigma_\alpha \left[\tau_1 h_q^\alpha - \tau_2 d_q^\alpha \right], \tag{D26}$$

where we have introduced the short-hand notation that for $\alpha = q, cl$ we have $\sigma_q = \frac{1}{2}\sigma_1$ and $\sigma_{cl} = \sigma_0$.

We expand the effective action in terms of the parameterized collective modes. The Hubbard-Stratonovich term has

$$S_{\text{HS}} = -\frac{2}{g_d} \sum_q \left[h_{-q}^{cl} h_q^q + d_{-q}^{cl} d_q^q \right], \tag{D27}$$

and is therefore diagonal in this representation. The quasiparticle contribution is

$$S_{\text{QP}} = \frac{i}{2} \sum_q \int_p |\chi_{\mathbf{p}}^d|^2 \mathrm{tr} \left\{ \check{\mathbb{G}}_0(p + \tfrac{1}{2}q)\sigma_\alpha \left[\tau_1 h_q^\alpha - \tau_2 d_q^\alpha \right] \check{\mathbb{G}}_0(p - \tfrac{1}{2}q)\sigma_\beta \left[\tau_1 h_{-q}^\beta - \tau_2 d_{-q}^\beta \right] \right\}. \tag{D28}$$

Consider the cross-coupling between the h and d modes. This involves a trace over the Green's functions with one vertex in the τ_1 channel and the other in the τ_2 channel. The only non-trivial contraction of the Nambu matrices must involve a τ_3 in one Green's function and a τ_0 in the other, and thus must be odd in ξ. As such, in the quasiclassical limit this goes as $\int d\xi \xi$ and will nearly vanish due to approximate particle-hole symmetry (more accurately, it is small in Δ/E_F). Therefore we neglect the cross coupling and see that the h and d modes decouple.

The action for each is then found to be

$$S_{dd} = \sum_q \left[-\frac{2}{g_d} d_{-q}^q d_q^{cl} + d_q^\alpha d_{-q}^\beta \frac{i}{2} \int_p |\chi_{\mathbf{p}}^d|^2 \mathrm{tr} \check{\mathbb{G}}_0(p + \tfrac{1}{2}q)\sigma_\alpha \tau_2 \check{\mathbb{G}}_0(p - \tfrac{1}{2}q)\sigma_\beta \tau_2 \right] \tag{D29a}$$

$$S_{hh} = \sum_q \left[-\frac{2}{g_d} h_{-q}^q h_q^{cl} + h_q^\alpha h_{-q}^\beta \frac{i}{2} \int_p |\chi_{\mathbf{p}}^d|^2 \mathrm{tr} \check{\mathbb{G}}_0(p + \tfrac{1}{2}q)\sigma_\alpha \tau_1 \check{\mathbb{G}}_0(p - \tfrac{1}{2}q)\sigma_\beta \tau_1 \right]. \tag{D29b}$$

Of these, the $q - q$ components are determined by fluctuation dissipation relation, so we focus on the $q - cl$ components. We have

$$S_{dd}^{q-cl} = \sum_q \left[-\frac{2}{g_d} d_q^q d_{-q}^{cl} + d_q^q d_{-q}^{cl} i \int_p |\chi_{\mathbf{p}}^d|^2 \mathrm{tr} \check{\mathbb{G}}_0(p + \tfrac{1}{2}q)\sigma_q \tau_2 \check{\mathbb{G}}_0(p - \tfrac{1}{2}q)\sigma_{cl} \tau_2 \right] \tag{D30a}$$

$$S_{hh}^{q-cl} = \sum_q \left[-\frac{2}{g_d} h_q^q h_{-q}^{cl} + h_q^q h_{-q}^{cl} i \int_p |\chi_{\mathbf{p}}^d|^2 \mathrm{tr} \check{\mathbb{G}}_0(p + \tfrac{1}{2}q)\sigma_q \tau_1 \check{\mathbb{G}}_0(p - \tfrac{1}{2}q)\sigma_{cl} \tau_1 \right]. \tag{D30b}$$

This reduces down to the calculation of the correlation functions

$$(L^R)_{ab}^{-1}(q) = -\frac{2}{g_d} \delta_{ab} + i \int_p |\chi_{\mathbf{p}}^d|^2 \mathrm{tr} \check{\mathbb{G}}_0(p - \tfrac{1}{2}q)\sigma_q \tau_a \check{\mathbb{G}}_0(p + \tfrac{1}{2}q)\sigma_{cl} \tau_b, \tag{D31}$$

and in particular we have the d-mode propagator in the $a = b = 2$ channel and the h-mode in the $a = b = 1$ channel.

We evaluate the trace over the Keldysh matrices to find

$$(L^R)^{-1}_{ab}(q) = -\frac{2}{g_d}\delta_{ab} + \frac{i}{2}\int_p |\chi^d_{\mathbf{p}}|^2 \text{tr}\left[\tau_b \hat{\mathbb{G}}^K(p - \frac{1}{2}q)\tau_a \hat{\mathbb{G}}^R(p + \frac{1}{2}q) + \tau_a \hat{\mathbb{G}}^K(p + \frac{1}{2}q)\tau_b \hat{\mathbb{G}}^A(p - \frac{1}{2}q)\right]. \tag{D32}$$

We evaluate this at center of mass momentum $\mathbf{q} = 0$, to simplify our analysis. In this case, the quasiclassical approximation may be invoked and we can average over the Fermi surface. This removes the d-wave form factors and gives

$$\frac{1}{\nu_F}(L^R)^{-1}_{ab}(\Omega, \mathbf{q} = 0) = -2\lambda_d^{-1}\delta_{ab} + \frac{i}{2}\int\frac{d\varepsilon}{2\pi}\int d\xi \text{tr}\left[\tau_b \hat{\mathbb{G}}^K(\varepsilon - \frac{\Omega}{2}, \xi)\tau_a \hat{\mathbb{G}}^R(\varepsilon + \frac{\Omega}{2}, \xi) + \tau_a \hat{\mathbb{G}}^K(\varepsilon + \frac{\Omega}{2}, \xi)\tau_b \hat{\mathbb{G}}^A(\varepsilon - \frac{\Omega}{2}, \xi)\right]. \tag{D33}$$

We can simplify slightly by shifting ε to get for the diagonal components

$$\frac{1}{\nu_F}(L^R)^{-1}_{aa}(\Omega, \mathbf{q} = 0) = -2\lambda_d^{-1} + \frac{i}{2}\int\frac{d\varepsilon}{2\pi}\int d\xi \tau_a \hat{\mathbb{G}}^K(\varepsilon, \xi)\tau_a\left[\hat{\mathbb{G}}^R(\varepsilon + \Omega, \xi) + \hat{\mathbb{G}}^A(\varepsilon - \Omega, \xi)\right]. \tag{D34}$$

In equilibrium we have

$$\hat{\mathbb{G}}^K(\varepsilon, \xi) = \tanh(\frac{\beta\varepsilon}{2})\left[\hat{\mathbb{G}}^R(\varepsilon, \xi) - \hat{\mathbb{G}}^A(\varepsilon, \xi)\right]. \tag{D35}$$

In order to accelerate integrals and improve convergence we fold the integration over $-\varepsilon$ and integrate only over positive ξ. The integrals over positive ξ only are permissible because all terms odd in ξ will not enter and therefore don't need to be cancelled. All terms in the given expression are either in the τ_0, τ_3, τ_1 channels. The Green's function trace will therefore involve traces of the terms $\tau_0^2, \tau_1^2, \tau_3^2, \tau_1, \tau_3, i\tau_2$. Of these, the last three will vanish and only the first three survive, which are the squares of each individual term and therefore the trace will kill all terms odd in ξ.

Thus, we evaluate this numerically as

$$\frac{1}{\nu_F}(L^R)^{-1}_{aa}(\Omega, \mathbf{q} = 0) = -2\lambda_d^{-1}$$
$$-\frac{1}{2i}\frac{1}{2\pi}\int_0^\infty d\varepsilon 2\int_0^\Lambda d\xi\left(\tau_a \hat{\mathbb{G}}^K(\varepsilon, \xi)\tau_a\left[\hat{\mathbb{G}}^R(\varepsilon + \Omega, \xi) + \hat{\mathbb{G}}^A(\varepsilon - \Omega, \xi)\right] + \tau_a \hat{\mathbb{G}}^K(-\varepsilon, \xi)\tau_a\left[\hat{\mathbb{G}}^R(-\varepsilon + \Omega, \xi) + \hat{\mathbb{G}}^A(-\varepsilon - \Omega, \xi)\right]\right). \tag{D36}$$

In particular, we plot the spectral functions

$$\mathcal{A}_{dd}(\Omega) = -\frac{1}{\pi}\Im L^R_{22}(\Omega, \mathbf{q} = 0) \tag{D37}$$

which are used to locate the collective mode resonances.

Appendix E: Dependence on Substrate Gap and Minigap

Here we briefly detail the dependence of the spectral functions on the substrate gap Δ_s and the minigap γ, shown in Fig. 7 and Fig. 8, respectively. We see in particular that for finite γ with $\Delta_s = 0$ the substrate acts as a reservoir and broadens the electronic spectral function. We then see no sharp mode in the d-wave channel, but instead it is replaced by an overdamped superconducting fluctuation. In the absence of strong substrate effects this mode will have a lifetime which scales as $\tau^{-1} \sim T - T_d$, as it condenses at $T = T_d$ [47]. By inducing a substrate gap we crossover from the fluctuation regime, with Azlamazov-Larkin type features, to the sharp collective mode outlined in the main text.

In Fig. 8 we explore the dependence of the spectral function on the minigap γ. We see that for small γ, the mode is not sharp since the minigap is small and there is considerable overlap between the continuum and bound state. As the minigap increases, we see the separation of the bound state improve as the spectral weight between the collective mode and conitnuum is suppressed.

Appendix F: f-Wave Pairing in Graphene

As a more involved and relevant application we consider the recent proposal by Chou, *et. al.* [29] that many graphene based superconductors realize a generically spin-triplet f-wave paired state. In particular, we argue that in this case, the system is also well suited for study via the collective-mode method we outline here.
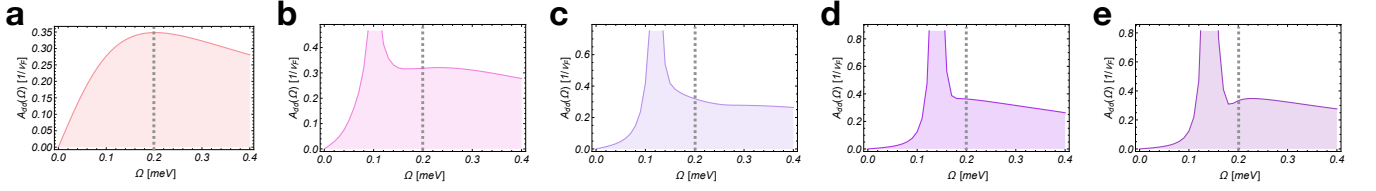
FIG. 7. Collective mode spectral function for different values of Δ_s at fixed $\gamma = .2\text{meV}$, $T = T_d^{(0)} = .344\text{meV}$, and $\Lambda = 30\text{meV}$. We plot the spectral function for $\Delta_s = 0, .1, .2, .5, 1.0\text{meV}$ in (a)-(e) respectively. We see the evolution from an overdamped superconducting fluctuation in (a) in to a sharp collective mode in (e). Dashed line indicates the value of γ in each plot, which is fixed at $\gamma = .2\text{meV}$.
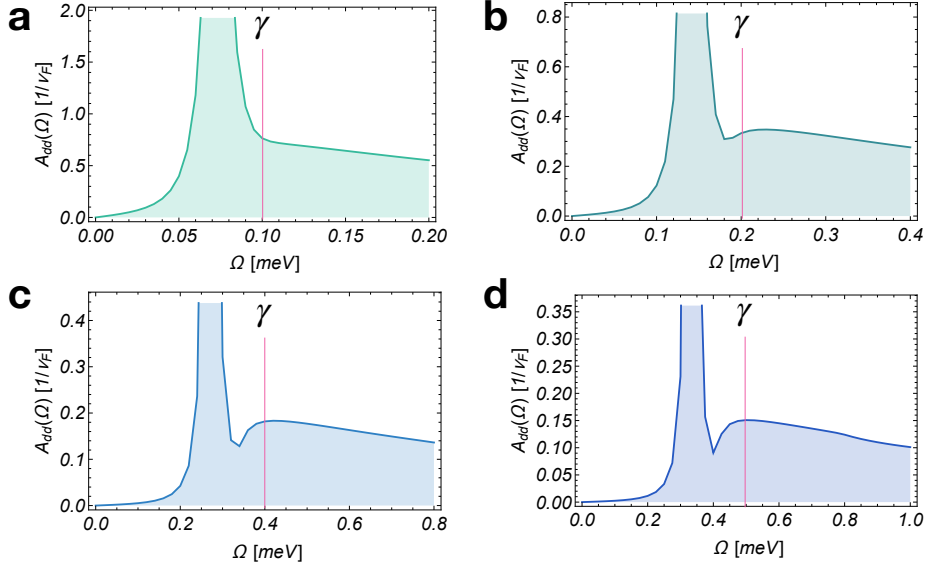
FIG. 8. Spectral function of proximity-induced Bardasis-Schrieffer collective mode for different strengths of the tunneling-induced minigap. We fix the substrate gap to be $\Delta_s = 1.0$ meV, and hold the cutoff $\Lambda = 30$ meV and BCS constant $\lambda_d^{-1} = 4.58658$, corresponding to an intrinsic critical temperature of $T_d^{(0)} = .344$ meV. We also fix the temperature $T = T_d^{(0)}$. We then study the spectral function while we vary the size of the tunneling rate γ from .1meV in (a) through .4meV in (d) in increments of .1 meV. The plots are shown over a frequency range from 0 to 2γ, and at $\Omega = \gamma$ we place a line as a guide to the eye, which indicates where the two-particle continuum formally begins.

In Ref. [29], it was argued that a nearby ferromagnetic critical point was the origin of pairing in many moiré graphene systems, and a simple spin-fermion model was employed to model these magnetization fluctuations. The interaction was decomposed into multiple pairing channels involving the spin ($\boldsymbol{\sigma}$), valley ($\boldsymbol{\rho}$), and sublattice ($\boldsymbol{\zeta}$) degrees of freedom, along with the usual particle-hole ($\boldsymbol{\tau}$) subspace (with their corresponding Pauli matrices indicated), and it was shown that generically the f-wave spin-triplet pairing dominated, within a BCS-type approximation.

We adopt this argument and focus on the dominant pairing. We use an effective description of graphene near charge neutrality with Bloch Hamiltonian

$$\mathcal{H}_0(\mathbf{k}) = \mathrm{v}_F(\rho_z\zeta_x k_x + \zeta_y k_y) - E_F, \tag{F1}$$

where v_F is the Fermi velocity and E_F is a Fermi level introduced to model the departure from perfect neutrality/perfect single-layer graphene dispersion.

The relevant pairing considered is in the spin-triplet channel, with order parameter (written here as $\boldsymbol{d}$ vector)

$$\boldsymbol{d} = g_f \int_{\mathbf{k}} \langle \psi_{-\mathbf{k}}^T \left(i\sigma_y \boldsymbol{\sigma} i\rho_y \right) \psi_{\mathbf{k}} \rangle. \tag{F2}$$

In contrast, a simple even-parity s-wave singlet pairing state has order parameter

$$\Delta = g_s \int_{\mathbf{k}} \langle \psi_{-\mathbf{k}}^T \left(-i\sigma_y \rho_x \right) \psi_{\mathbf{k}} \rangle. \tag{F3}$$

Following the simpler example described in the text, we will consider proximity inducing an s-wave singlet gap in this channel, and look for the collective modes in the corresponding f-wave triplet channels.

We describe the paired system in terms of the Nambu spinor

$$\Psi_{\mathbf{k}} = \begin{pmatrix} \psi_{\mathbf{k}} \\ (i\sigma_y)\rho_x(\psi_{-\mathbf{k}}^{\dagger})^T \end{pmatrix}. \tag{F4}$$

Here we consider pairing between Kramer's doublets. Note that in the presence of the valley pseudospin, time-reversal symmetry acts on an electron in real space as $\mathcal{T} = i\sigma_y\rho_x K$ where K is the usual complex conjugation. We maintain $\mathcal{T}^2 = -1$.

In the absence of the substrate self-energy, the quasiparticle dynamics are governed by the Bogoliubov-de Gennes Hamiltonian

$$\hat{\mathcal{H}}_{\mathrm{BdG}}(\mathbf{k}) = \begin{pmatrix} \mathcal{H}_0(\mathbf{k}) & \rho_z \boldsymbol{\sigma} \cdot \overline{\mathbf{d}}(x) \\ \rho_z \boldsymbol{\sigma} \cdot \mathbf{d}(x) & -\rho_x \mathcal{H}_0^T(-\mathbf{k})\rho_x \end{pmatrix}. \tag{F5}$$

We have allowed for a slowly-varying triplet field $\mathbf{d}$, relevant for the fluctuation effects discussed later. We assume pairing interaction in the f-wave channel, but a proximity induced gap in the s-wave channel.

We note the following relation

$$- \rho_x \mathcal{H}_0^T(-\mathbf{k})\rho_x = -\mathcal{H}_0(\mathbf{k}). \tag{F6}$$

We also have $[\boldsymbol{\sigma}, \mathcal{H}_0(\mathbf{k})] = [\rho_z, \mathcal{H}_0(\mathbf{k})] = 0$. In this way, the f-wave pairing commutes with single-particle Hamiltonian, making an interesting connection with the recently introduced concept of superconducting fitness [31].

The substrate self-energy is written in the Nambu basis as

$$\hat{\boldsymbol{\Sigma}}^R(\epsilon) = -\frac{\gamma}{2}\left(\frac{\varepsilon - \Delta_s \tau_1}{\sqrt{\Delta_s^2 - (\varepsilon + i0^+)^2}} \right) \tag{F7}$$

with substrate gap Δ_s chosen to be real, and $\gamma = 2\pi\nu_s|\mathbf{t}|^2$ the minigap induced by the tunneling into the substrate and back. Note that the valley matrix ρ_x is absorbed into the Nambu spinor.

We now determine the pair spectral function in the f-wave channel, which the system would otherwise condense into. We take inverse BCS pairing constant in the relevant channel of $\frac{1}{g_f}$.

One of the main differences with the previously considered d-wave pairing model is that, due to the miniscule spin-orbit coupling in graphene, the three triplet spin polarizations are degenerate. As a result, we expect that we should find not one, but **three** Bardasis-Schrieffer collective modes, each with a different spin polarization. While at the level of Gaussian fluctuations, this is true, the story does become more interesting and complicated if the second transition temperature is crossed. In this case, it remains to be seen whether the condensate spontaneously breaks both time-reversal and spin-rotation symmetry, or if a more complicated scenario involving strong spin fluctuations is favored. This is a very interesting possibility, which we will leave to future works.

We again employ the Keldysh framework to describe the collective mode fluctuations. The retarded/advanced propagators are found using the Bogoliubov-de Gennes Hamiltonian described above, and we find

$$\mathbb{G}^R(\epsilon, \mathbf{p}) = \left(\epsilon - \mathcal{H}_{\mathrm{BdG}}(\mathbf{p}) - \hat{\boldsymbol{\Sigma}}^R(\epsilon) \right)^{-1}. \tag{F8}$$

We clarify, to avoid confusion, that here the $\boldsymbol{\sigma}$ matrices now characterize the spin degree of freedom, whereas previously they were the Keldysh space. We here leave the Keldysh indices explicit to avoid confusion. To obtain the collective mode propagator, we expand to second order in the fluctuating $\mathbf{d}$-wave order. We find retarded generalized RPA contribution in the Bardasis-Scrhrieffer (out-of-phase pairing) channel, now spin resolved,

$$\Pi_{lm}^R(q) = \frac{i}{4}\int_p \mathrm{tr}\left[\boldsymbol{\sigma}_l\rho_z\tau_y\hat{\mathbb{G}}_0^R(p+\frac{q}{2})\boldsymbol{\sigma}_m\rho_z\tau_y\hat{\mathbb{G}}_0^K(p-\frac{q}{2}) + \boldsymbol{\sigma}_m\rho_z\tau_y\hat{\mathbb{G}}_0^K(p+\frac{q}{2})\boldsymbol{\sigma}_l\rho_z\tau_y\hat{\mathbb{G}}_0^A(p-\frac{q}{2}) \right]. \tag{F9}$$

We have an additional factor of 2 since we are now dealing with the full particle-hole doubled Nambu space to incorporate the triplet order as well. In this case, the propagator is the normal-state Hamiltonian, plus the substrate self-energy, so that

$$\hat{\mathbb{G}}_0^R(p) = \left(\epsilon - \tau_3\mathcal{H}_0(\mathbf{p}) - \hat{\Sigma}(\epsilon) \right)^{-1} \tag{F10}$$

where we have explicitly used the fact that the normal-state part of the BdG Hamiltonian is τ_3 times the reduced Bloch Hamiltonian $\mathcal{H}_0(\mathbf{k})$. The s-wave pairing is captured by the off-diagonal part of $\boldsymbol{\Sigma}$.

In this case the total pair propogator for the f-wave fluctuations is, at $\mathbf{q} = 0$,

$$L_{lm}^R(\Omega, \mathbf{q} = 0) = -\frac{2}{g_f}\delta_{lm} + \Pi_{lm}^R(\Omega). \tag{F11}$$

In the absence of magnetic ordering this is isotropic in spin space, and indeed in the s-wave proximized state we find that $[\boldsymbol{\sigma}, \hat{\mathbb{G}}] = 0$, so that the trace over spin index yields a Kronecker delta. Evidently, we can diagonalize the Bloch Hamiltonian, and write in terms of the energy eigenvalues alone, which are degenerate for the two valleys, as $\xi_{\mathbf{p},\zeta}$ with

$$\xi_{\mathbf{p},\pm} = -E_F \pm \mathrm{v}_F|\mathbf{p}|. \tag{F12}$$

We can perform the trace over spin and valley indices to get $\Pi_{lm}^R(\Omega) = \delta_{lm}\Pi^R(\Omega)$ with

$$\Pi^R(\Omega) = \frac{i}{2}\int_p \sum_{\zeta=\pm} \mathrm{tr}\left[\tau_y \hat{\mathbb{G}}_0^R(\omega + \frac{\Omega}{2}, \xi_{\mathbf{p},\zeta})\tau_y \hat{\mathbb{G}}_0^K(\omega - \frac{\Omega}{2}, \xi_{\mathbf{p},\zeta}) + \tau_y \hat{\mathbb{G}}_0^K(\omega + \frac{\Omega}{2}, \xi_{\mathbf{p},\zeta})\tau_y \hat{\mathbb{G}}_0^A(\omega - \frac{\Omega}{2}, \xi_{\mathbf{p},\zeta})\right]. \tag{F13}$$

Furthermore, one can diagonalize the remaining degrees of freedom (sublattice $\boldsymbol{\zeta}$) by passing to the energy eigenbasis of the normal state Hamiltonian. We find as $\mathbf{q} \to 0$ a further simplification since the pairing vertices also commute with the resulting band indices, so that we can perform the trace over ζ as well. We then find

$$\Pi^R(\Omega) = i \sum_{\zeta=\pm 1}\int_p \mathrm{tr}\hat{\mathbb{G}}_0^K(\epsilon, \xi_{\mathbf{p},\zeta})\left[\tau_y \hat{\mathbb{G}}_0^R(\epsilon + \Omega, \xi_{\mathbf{p},\zeta})\tau_y + \tau_y \hat{\mathbb{G}}_0^A(\epsilon - \Omega, \xi_{\mathbf{p},\zeta})\tau_y\right]. \tag{F14}$$

The trace now is only over the Nambu index, which is the only remaining degree of freedom. Furthermore, this will ensure that the integrand only depends on the kinetic energy through a dependence on $\xi_{\mathbf{p},\zeta}^2$. We can evaluate functions of the form

$$\sum_{\zeta=\pm 1}\int \frac{d^2p}{(2\pi)^2}\mathcal{F}(\xi_{\mathbf{p},\zeta}^2) = \int d\xi \nu(\xi)\mathcal{F}(\xi^2), \tag{F15}$$

with the aggregated density of states being

$$\nu(\xi) = \begin{cases} \frac{(\xi+E_F)}{2\pi\mathrm{v}_F^2} & \xi > -E_F \\ \frac{(-\xi+E_F)}{2\pi\mathrm{v}_F^2} & \xi < -E_F. \end{cases} \tag{F16}$$

Importantly, we find a non-zero density of states at the Fermi level, with $\nu_F = E_F/(2\pi\mathrm{v}_F^2)$. We will here make the quasiclassical approximation, though in the likely event that E_F is small, this should be revisited, since it is likely that particle-hole symmetry will be strongly violated.

In the limit of quasiclassical approximation, we find indeed that this integral now exactly recovers to the form previously investigated, and we therefore conclude that the up to numerical factors of 2 and such, the phenomenology is the same besides the emergence of three modes in this case. Studying these collective modes in even greater detail is an interesting topic which we reserve for later study.

[1] J. Linder and J. Robinson, Superconducting Spintronics, Nat. Phys. **11**, 307 (2015).

[2] N. Poniatowski, J. Curtis, C. Bøttcher, V. Galitski, A. Yacoby, P. Narang, and E. Demler, Surface cooper pair spin waves in triplet superconductors (2021), arXiv:2112.12146 [cond-mat.supr-con].

[3] G. Yang, C. Ciccarelli, and J. W. A. Robinson, Boosting spintronics with superconductivity, APL Materials **9**, 050703 (2021).

[4] J. Alicea, New directions in the pursuit of Majorana fermions in solid state systems, Reports on Progress in Physics **75**, 076501 (2012).

[5] C. Nayak, S. H. Simon, A. Stern, M. Freedman, and S. Das Sarma, Non-abelian anyons and topological quantum computation, Rev. Mod. Phys. **80**, 1083 (2008).

[6] P. Zareapour, A. Hayat, S. Zhao, M. Kreshchuk, A. Jain, D. Kwok, N. Lee, S.-W. Cheong, Z. Xu, A. Yang, G. Gu, S. Jia, R. Cava, and K. Burch, Proximity-induced high-

temperature superconductivity in the topological insulators Bi_2Se_3 and Bi_2Te_3 , Nature Comm. **3**, 1056 (2012).

[7] M. Sigrist, Broken time reversal symmetry in unconventional superconductors, Physica C: Superconductivity **341-348**, 695 (2000).

[8] S. Maiti and P. J. Hirschfeld, Collective modes in superconductors with competing *s*- and *d*-wave interactions, Phys. Rev. B **92**, 094506 (2015).

[9] K. A. Musaelian, J. Betouras, A. V. Chubukov, and R. Joynt, Mixed-symmetry superconductivity in two-dimensional fermi liquids, Phys. Rev. B **53**, 3598 (1996).

[10] V. Stanev and Z. Tesanović, Three-band superconductivity and the order parameter that breaks time-reversal symmetry, Phys. Rev. B **81**, 134522 (2010).

[11] S. K. Ghosh, M. Smidman, T. Shang, J. F. Annett, A. D. Hillier, J. Quintanilla, and H. Yuan, Recent progress on superconductors with time-reversal symmetry breaking, Journal of Physics: Condensed Matter **33**, 033001 (2020).

[12] Wysokiǹski, K.I., Time Reversal Symmetry Breaking Superconductors: Sr_2RuO_4 and Beyond, Condens. Matter **4**, 47 (2019).

[13] P. Narang, C. Garcia, and C. Felser, The topology of electronic band structures, Nature Materials **20**, 293 (2020).

[14] L. Olde Olthoff, L. Johnsen, J. Robinson, and J. Linder, Controllable Enhancement of *p*-Wave Superconductivity via Magnetic Coupling to a Conventional Superconductor , Phys. Rev. Lett. **127**, 267001 (2021).

[15] L. Schwarz, B. Fauseweh, N. Tsuji, N. Cheng, N. Bittner, H. Krull, M. Berciu, G. S. Uhrig, A. P. Schnyder, S. Kaiser, and D. Manske, Classification and characterization of nonequilibrium Higgs modes in unconventional superconductors, Nature Communications **11**, 287 (2020).

[16] L. Schwarz and D. Manske, Theory of driven Higgs oscillations and third-harmonic generation in unconventional superconductors, Phys. Rev. B **101**, 184519 (2020).

[17] N. R. Poniatowski, J. B. Curtis, A. Yacoby, and P. Narang, Spectroscopic signatures of time-reversal symmetry breaking superconductivity (2021), arXiv:2103.05641 [cond-mat.supr-con].

[18] R. Matsunaga, N. Tsuji, H. Fujita, A. Sugioka, K. Makise, Y. Uzawa, H. Terai, Z. Wang, H. Aoki, and R. Shimano, Light-induced collective pseudospin precession resonating with Higgs mode in a superconductor, Science **345**, 1145 (2014), https://science.sciencemag.org/content/345/6201/1145.full.pdf.

[19] H. Uematsu, T. Mizushima, A. Tsuruta, S. Fujimoto, and J. A. Sauls, Chiral Higgs mode in nematic superconductors, Phys. Rev. Lett. **123**, 237001 (2019).

[20] B. Nosarzewski, B. Moritz, J. Freericks, A. Kemper, and T. Devereaux, Amplitude mode oscillations in pump-probe photoemission spectra from a *d*-wave superconductor, Phys. Rev. B **96**, 184518 (2017).

[21] L. Tewordt, Collective order parameter modes and spin fluctuations for spin-triplet superconducting state in Sr_2RuO_4, Phys. Rev. Lett. **83**, 1007 (1999).

[22] A. Balatsky, P. Kumar, and J. Schrieffer, Clapping modes in unconventional superconductors, Physica C **341**, 807 (2000).

[23] S.-Z. Lin, Ground state, collective mode, phase soliton and vortex in multiband superconductors, Journal of Physics: Condensed Matter **26**, 493202 (2014).

[24] M. Marciani, L. Fanfarillo, C. Castellani, and L. Benfatto, Leggett modes in iron-based superconductors as a probe of time-reversal symmetry breaking, Phys. Rev. B **88**, 214508 (2013).

[25] Y. Tanaka and S. Kashiwaya, Theory for tunneling spectroscopy of anisotropic superconductors, Phys. Rev. B **53**, 9371 (1996).

[26] S. Kashiwaya, Y. Tanaka, M. Koyanagi, and K. Kajimura, Theory for tunneling spectroscopy of anisotropic superconductors, Phys. Rev. B **53**, 2667 (1996).

[27] S. Kashiwaya and Y. Tanaka, Tunnelling effects on surface bound states in unconventional superconductors, Rep. Prog. Phys. **63**, 1641 (2000).

[28] A. Bardasis and J. R. Schrieffer, Excitons and plasmons in superconductors, Phys. Rev. **121**, 1050 (1961).

[29] Y.-Z. Chou, F. Wu, J. Sau, and S. Das Sarma, Correlation-induced triplet pairing superconductivity in graphene-based moiré systems, Phys. Rev. Lett. **127**, 217001 (2021).

[30] In particular, we mean to exclude scenarios where the interface itself breaks symmetries and allows the *s*-wave substrate order to linearly couple to the intrinsic order, as may occur for instance with a p_z order parameter which is protected by the horizontal mirror-plane symmetry. In this case, the relevant symmetry is broken and the two order parameters will hybridize to form a parity-mixed state, requiring a more complicated analysis which includes a re-evaluation of the mean-field state. While the situation is more complicated, this may be a potentially interesting route for future study as well. We thank Jacob Linder for highlighting this interesting direction.

[31] A. Ramires, D. Agterberg, and M. Sigrist, Tailoring T_c by symmetry principles: The concept of superconducting fitness, Phys. Rev. B **98**, 024501 (2018).

[32] D. Scalapino, Pair tunnelling as a probe of fluctuations in superconductors, Phys. Rev. Lett. **24**, 1052 (1970).

[33] A. Abrikosov, L. Gor'kov, and I. Dzyaloshinskii, *Methods of Quantum Field Theory In Statistical Physics* (Pergamon Press, 1965).

[34] M. Sigrist, K. Kuboki, P. A. Lee, A. J. Millis, and T. M. Rice, Influence of twin boundaries on Josephson junctions between high-temperature and conventional superconductors, Phys. Rev. B **53**, 2835 (1996).

[35] W. Belzig, C. Bruder, and M. Sigrist, Quasiclassical theory of twin boundaries in high- T_c superconductors, Phys. Rev. Lett. **80**, 4285 (1998).

[36] K. Kuboki and M. Sigrist, Proximity-induced time-reversal symmetry breaking at Josephson jnctions between *d*-wave superconductors, Czechoslovak Journal of Physics **46**, 1039 (1996).

[37] A. Huck, A. van Otterlo, and M. Sigrist, Time-reversal symmetry breaking and spontaneous currents in *s*-wave/normal-metal/*d*-wave superconductor sandwiches, Phys. Rev. B **56**, 14163 (1997).

[38] K. Kuboki and M. Sigrist, Proximity-induced time-reversal symmetry breaking at Josephson junctions between unconventional superconductors, Journal of the Physical Society of Japan **65**, 361 (1996).

[39] S.-Z. Lin, Josephson effect between a two-band superconductor with s++ or s± pairing symmetry and a conventional s-wave superconductor, Phys. Rev. B **86**, 014510 (2012).

[40] O. Can, T. Tummuru, R. P. Day, I. Elfimov, A. Damascelli, and M. Franz, High-temperature topological superconductivity in twisted double-layer copper oxides, Nature Physics **17**, 519 (2021).

[41] P. A. Volkov, J. H. Wilson, and J. H. Pixley, Magic angles and current-induced topology in twisted nodal supercon-ductors (2020), arXiv:2012.07860 [cond-mat.supr-con].

[42] S. Y. F. Zhao, N. Poccia, X. Cui, P. A. Volkov, H. Yoo, R. Engelke, Y. Ronen, R. Zhong, G. Gu, S. Plugge, T. Tummuru, M. Franz, J. H. Pixley, and P. Kim, Emergent Interfacial Superconductivity between Twisted Cuprate Superconductors (2021), 2108.13455.

[43] Y. Yerin and A. Omelyanchouk, Frustration phenom-ena in josephson point contacts between single-band and three-band superconductors, Low Temp. Phys. **40**, 943 (2014).

[44] Y. Yerin, A. Kiyko, A. Omelyanchouk, and E. Il'ichev, Josephson systems based on ballistic point contacts be-tween single-band and multi-band superconductors, Low Temp. Phys. **41**, 885 (2015).

[45] C. J. Trimble, M. T. Wei, N. F. Q. Yuan, S. S. Kalantre, P. Liu, H.-J. Han, M. G. Han, Y. Zhu, J. J. Cha, L. Fu, and J. R. Williams, Josephson detection of time-reversal symmetry broken superconductivity in snte nanowires, npj Quant. Mat. **6**, 61 (2021).

[46] In particular, in the mean-field limit the two-particle spectral function is completely fixed by the single-particle density-of-states, and this exhibits a weak singularity at the gap edge which may be confused with a collective mode if the resonance lies to close to the continuum.

[47] A. Larkin and A. Varlamov, *Theory of Fluctuations in Superconductors* (Oxford University Press, Oxford, 2005).

[48] A. Kadin and A. Goldman, Pair-field susceptibility and superconducting tunneling: A macroscopic approach, Phys. Rev. B **25**, 6701 (1982).

[49] A. Goldman, The Order Parameter Susceptibility and Collective Modes of Superconductors, J. Supercond. **19**, 317 (2006).

[50] G.-H. Lee, K.-F. Huang, D. Efetov, D. Wei, S. Hart, T. Taniguchi, K. Watanabe, A. Yacoby, and P. Kim, In-ducing superconducting correlation in quantum Hall edge states, Nat. Phys. **13**, 693 (2017).

[51] L. Bretheau, J.-J. Wang, R. Pisoni, K. Watanabe, T. Taniguchi, and P. Jarillo-Herrero, Tunnelling spec-troscopy of Andreev states in graphene, Nat. Phys. **13**, 756 (2017).

[52] J. Li, H.-B. Leng, H. Fu, K. Watanabe, T. Taniguchi, X. Liu, C.-X. Liu, and J. Zhu, Superconducting proximity effect in a transparent van der Waals superconductor-metal junction, Phys. Rev. B **101**, 195405 (2020).

[53] R. Moriya, N. Yabuki, and T. Machida, Superconduct-ing proximity effect in a NbSe$_2$/graphene van der Waals junction, Phys. Rev. B **101**, 054503 (2020).

[54] E. Wolf, *Principles of Electron Tunneling Spectroscopy* (Oxford University Press, 2011).

[55] L. Vitali, M. A. Schneider, K. Kern, L. Wirtz, and A. Ru-bio, Phonon and plasmon excitation in inelastic electron tunneling spectroscopy of graphite, Phys. Rev. B **69**, 121414(R) (2004).

[56] T. Balashov, A. Takács, W. Wulfhekel, and J. Kirschner, Magnon Excitation with Spin-Polarized Scanning Tun-neling Microscopy, Phys. Rev. Lett. **97**, 187201 (2006).

[57] P. Hlobil, J. Jandke, W. Wulfhekel, and J. Schmalian, Tracing the Electronic Pairing Glue in Unconventional Superconductors via Inelastic Scanning Tunneling Spec-troscopy, Physical Review Letters **118**, 167001 (2017), 1603.05288.

[58] J. Jandke, P. Hlobil, M. Schackert, W. Wulfhekel, and J. Schmalian, Coupling to real and virtual phonons in tunneling spectroscopy of superconductors, Physical Re-view B **93**, 060505 (2016), 1504.01932.

[59] M. Norman, H. Ding, H. Fretwell, M. Randeria, and J. Campuzano, Extraction of the electron self-energy from angle-resolved photoemission data: Application to Bi$_2$Sr$_2$CaCu$_2$O$_{8+x}$, Phys. Rev. B **60**, 7585 (1999).

[60] T. Valla, A. Fedorov, P. Johnson, and S. Hulbert, Many-Body Effects in Angle-Resolved Photoemission: Quasi-particle Energy and Lifetime of a Mo(110) Surface State, Phys. Rev. Lett. **83**, 2085 (1999).

[61] P. Hoffman, I. Sklyadneva, E. Rienks, and E. Chulkov, Electronphonon coupling at surfaces and interfaces, New J. Phys. **11**, 125005 (2009).

[62] T. Böhm, A. F. Kemper, B. Moritz, F. Kretzschmar, B. Muschler, H.-M. Eiter, R. Hackl, T. P. Devereaux, D. J. Scalapino, and H.-H. Wen, Balancing Act: Evidence for a Strong Subdominant *d*-Wave Pairing Channel in Ba$_{0.6}$K$_{0.4}$Fe$_2$As$_2$, Phys. Rev. X **4**, 041046 (2014).

[63] T. P. Devereaux and R. Hackl, Inelastic light scattering from correlated electrons, Reviews of Modern Physics **79**, 175 (2007), cond-mat/0607554.

[64] D. J. Scalapino and T. P. Devereaux, Collective d-wave exciton modes in the calculated Raman spectrum of Fe-based superconductors, Physical Review B **80**, 140512 (2009), 0904.1973.

[65] B. T. Zhou, N. F. Q. Yuan, H.-L. Jiang, and K. T. Law, Ising superconductivity and Majorana fermions in transition-metal dichalcogenides, Physical Review B **93**, 180501 (2016), 1510.06289.

[66] R. Wakatsuki and K. T. Law, Proximity effect and Ising superconductivity in superconductor/transition metal dichalcogenide heterostructures, arXiv (2016), 1604.04898.

[67] J. M. Lu, O. Zheliuk, I. Leermakers, N. F. Q. Yuan, U. Zeitler, K. T. Law, and J. T. Ye, Evidence for two-dimensional Ising superconductivity in gated MoS2, Sci-ence **350**, 1353 (2015), 1506.07620.

[68] Y. Saito, Y. Nakamura, M. S. Bahramy, Y. Kohama, J. Ye, Y. Kasahara, Y. Nakagawa, M. Onga, M. Toku-naga, T. Nojima, Y. Yanase, and Y. Iwasa, Superconduc-tivity protected by spinvalley locking in ion-gated MoS$_2$, Nature Physics **12**, 144 (2016), 1506.04146.

[69] X. Xi, Z. Wang, W. Zhao, J.-H. Park, K. T. Law, H. Berger, L. Forr, J. Shan, and K. F. Mak, Ising pairing in superconducting NbSe2 atomic layers, Nature Physics **12**, 139 (2016), 1507.08731.

[70] J. Lu, O. Zheliuk, Q. Chen, I. Leermakers, N. E. Hussey, U. Zeitler, and J. Ye, Full superconducting dome of strong Ising protection in gated monolayer WS$_2$, Pro-ceedings of the National Academy of Sciences **115**, 201716781 (2018), 1703.06369.

[71] E. Sajadi, T. Palomaki, Z. Fei, W. Zhao, P. Be-ment, C. Olsen, S. Luescher, X. Xu, J. A. Folk, and D. H. Cobden, Gate-induced superconductivity in a monolayer topological insulator, Science **362**, 922 (2018), https://www.science.org/doi/pdf/10.1126/science.aar4426.

[72] V. Fatemi, S. Wu, Y. Cao, L. Bretheau, Q. D. Gibson, K. Watanabe, T. Taniguchi, R. J. Cava, and P. Jarillo-Herrero, Electrically tunable low-density superconductiv-ity in a monolayer topological insulator, Science **362**, 926 (2018).

[73] V. Crpel and L. Fu, Spin-triplet superconductiv-

ity from interband effect in doped insulators (2021), arXiv:2103.12060 [cond-mat.supr-con].

[74] Y. Cao, V. Fatemi, S. Fang, K. Watanabe, T. Taniguchi, E. Kaxiras, and P. Jarillo-Herrero, Unconventional superconductivity in magic-angle graphene superlattices, Nature **556**, 43 (2018).

[75] J. M. Park, Y. Cao, K. Watanabe, T. Taniguchi, and P. Jarillo-Herrero, Tunable strongly coupled superconductivity in magic-angle twisted trilayer graphene, Nature **590**, 249 (2021).

[76] M. Oh, K. P. Nuckolls, D. Wong, R. L. Lee, X. Liu, K. Watanabe, T. Taniguchi, and A. Yazdani, Evidence for unconventional superconductivity in twisted bilayer graphene (2021), arXiv:2109.13944 [cond-mat.supr-con].

[77] H. Kim, Y. Choi, C. Lewandowski, A. Thomson, Y. Zhang, R. Polski, K. Watanabe, T. Taniguchi, J. Alicea, and S. Nadj-Perge, Spectroscopic signatures of strong correlations and unconventional superconductivity in twisted trilayer graphene (2021), arXiv:2109.12127 [cond-mat.mes-hall].

[78] Y. Yu, L. Ma, P. Cai, R. Zhong, C. Ye, J. Shen, G. D. Gu, X. H. Chen, and Y. Zhang, High-temperature superconductivity in monolayer $Bi_2Sr_2CaCu_2O_{8+\delta}$, Nature **575**, 156 (2019).

[79] K. Tanigaki, T. Ebbesen, S. Saito, J. Mizuki, J. Tsai, Y. Kubo, and S. Kuroshima, Superconductivity at 33 K in Cs_xRb_yC60, Nature **352**, 222 (1991).

[80] T. Cea, C. Castellani, and L. Benfatto, Nonlinear optical effects and third-harmonic generation in superconductors: Cooper pairs versus Higgs mode contribution, Phys. Rev. B **93**, 180507 (2016).

[81] R. Shimano and N. Tsuji, Higgs mode in superconductors, Annual Review of Condensed Matter Physics **11**, 103 (2020), https://doi.org/10.1146/annurev-conmatphys-031119-050813.

[82] P. B. Littlewood and C. M. Varma, Gauge-invariant theory of the dynamical interaction of charge density waves and superconductivity, Phys. Rev. Lett. **47**, 811 (1981).

[83] M.-A. Méasson, Y. Gallais, M. Cazayous, B. Clair, P. Rodière, L. Cario, and A. Sacuto, Amplitude Higgs mode in the 2h-NbSe$_2$ superconductor, Phys. Rev. B **89**, 060503 (2014).

[84] A. C. Potter and P. A. Lee, Engineering a $p + ip$ superconductor: Comparison of topological insulator and Rashba spin-orbit-coupled materials, Phys. Rev. B **83**, 184520 (2011).

[85] D. Chevallier, P. Simon, and C. Bena, From Andreev bound states to Majorana fermions in topological wires on superconducting substrates: A story of mutation, Phys. Rev. B **88**, 165401 (2013).

[86] T. Stanescu, J. Sau, R. Lutchyn, and S. Das Sarma, Proximity effect at the superconductortopological insulator interface, Phys. Rev. B **81**, 241310(R) (2010).

[87] A. Kamenev, *Field Theory of Non-Equilibrium Systems* (Cambridge University Press, 2011).